FOR OFFICIAL USE ONLY

JPRS L/8415

23 April 1979

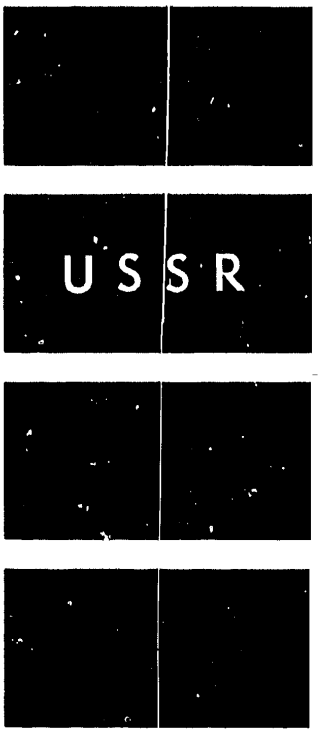

TRANSLATIONS ON USSR SCIENCE AND TECHNOLOGY
PHYSICAL SCIENCES AND TECHNOLOGY
(FOUO 23/79)

U. S. JOINT PUBLICATIONS RESEARCH SERVICE

FOR OFFICIAL USE ONLY

NOTE

JPRS publications contain information primarily from foreign newspapers, periodicals and books, but also from news agency transmissions and broadcasts. Materials from foreign-language sources are translated; those from English-language sources are transcribed or reprinted, with the original phrasing and other characteristics retained.

Headlines, editorial reports, and material enclosed in brackets [] are supplied by JPRS. Processing indicators such as [Text] or [Excerpt] in the first line of each item, or following the last line of a brief, indicate how the original information was processed. Where no processing indicator is given, the information was summarized or extracted.

Unfamiliar names rendered phonetically or transliterated are enclosed in parentheses. Words or names preceded by a question mark and enclosed in parentheses were not clear in the original but have been supplied as appropriate in context. Other unattributed parenthetical notes within the body of an item originate with the source. Times within items are as given by source.

The contents of this publication in no way represent the policies, views or attitudes of the U.S. Government.

APPROVED FOR RELEASE: 2007/02/09: CIA-RDP82-00850R000100040051-0

JPRS L/8415

23 April 1979

TRANSLATIONS ON USSR SCIENCE AND TECHNOLOGY
PHYSICAL SCIENCES AND TECHNOLOGY

(FOUO 23/79)

CONTENTS

CONTENTS (Continued) Page

PHYSICS

UDC 621.384.326

THE INFLUENCE OF OPTICAL SYSTEM ABERRATIONS ON THE MAIN PARAMETERS OF A THERMAL SCANNING VIEWER

Leningrad OPTIKO-MEKHANICHESKAYA PROMYSHLENNOST' in Russian No 11, 1978 pp 3-5

[Article by B.V. Ukhov, V.G. Klochkova, D.N. Krasnikov and S.M. Benza, manuscript received 16 Nov 77]

[Text] Questions related to the influence of the aberrations of the optical system of a thermal viewer on the angular resolving power and the signal to noise ratio are treated. Quantitative results are derived for various values of the time constant of the photodetector.

We shall assume that the thermal viewer observes an object which takes the form of two infinitely long strips, perpendicular to the direction of the line scanning. The width of these strips and the spacing between them corresponds to the instantaneous viewing angle of the thermal viewer, which we shall assume to be equal with respect to the line and frame. Let the x axis coincide with the direction of the line by line scanning, while the y axis corresponds to the frame scanning direction. We shall attempt to take into account the influence of the dimensions of the effective circle of confusion of the optical system on the waveform of the amplifier output signal and the basic parameters of the equipment.

In a real optical system, aberrations and diffraction scattering [1] wash out the images, where this blurring can be characterized by a scattering function h(x, y, x', y'). According to the literature [1], the distribution of the irradiance E(x, y) in the image plane of the optical system for the case of an irradiance $E_1(x', y')$ in the objective field is determined by means of the convolution integral:

$$E(x, y) = \int_{-\infty}^{\infty} \int_{-\infty}^{\infty} E_1(x', y')\, h(x, y, x', y')\, dx'\, dy'.$$

We shall approximate the scattering function with the gaussian function, something which is justified with a sufficient degree of precision for many actual optical systems:

$$h(x, y, x', y') = \frac{\gamma^2}{2\pi} e^{-\frac{\gamma^2[(x-x')^2+(y-y')^2]}{2}}.$$

In this case, the distribution of the irradiance, corresponding to the object in the form of one strip, will be defined by the expression:

$$E(x, y) = \frac{\gamma^2}{2\pi} B \int_{-a/2}^{a/2} \int_{-\infty}^{\infty} e^{-\frac{\gamma^2[(x-x')^2+(y-y')^2]}{2}} \times$$
$$\times dx'\, dy' = \frac{B}{2}\left\{\Phi\left[\gamma\left(x+\frac{a}{2}\right)\right] - \Phi\left[\gamma\left(x-\frac{a}{2}\right)\right]\right\},$$

where $\Phi(z) = \frac{2}{\sqrt{2\pi}} \int_0^z e^{-\frac{u^2}{2}}\, du$ is the probability integral; B is a constant; a is the size of the area of the photodetector.

The sensitive element of the photodetector observes the image by virtue of moving the latter along the x axis. This means the change in the irradiance of the receiver area E(x, t) with respect to time has the form [1]:

$$E(x, t) = E(x - vt) = \frac{B}{2}\left\{\Phi\left[\gamma\left(x - vt + \frac{a}{2}\right)\right] - \right.$$
$$\left. - \Phi\left[\gamma\left(x - vt - \frac{a}{2}\right)\right]\right\},$$

where v is the rate of travel of the image with respect to the receiver area.

The signal level at the output of an inertialess photodetector with uniform sensitivity ε over the area is:

$$I(t) = \frac{B\varepsilon}{2} \frac{1}{a^2} \int_{-\frac{a}{2}}^{\frac{a}{2}} \int_{-\frac{a}{2}}^{\frac{a}{2}} E(x, t)\, dx\, dy =$$
$$= \frac{B\varepsilon}{2a}\left\{(a + vt)\,\Phi[\gamma(a + vt)] - 2vt\Phi(\gamma vt) + \right.$$
$$+ (a - vt)\,\Phi[\gamma(a - vt)] +$$
$$+ \frac{2}{\sqrt{2\pi}} \frac{1}{\gamma} \exp\left[-\frac{\gamma^2}{2}(a + vt)^2\right] -$$
$$\left. - \frac{4}{\sqrt{2\pi}} \frac{1}{\gamma} \exp\left(\frac{\gamma^2 v^2 t^2}{2}\right) + \frac{2}{\sqrt{2\pi}} \frac{1}{\gamma} \exp\left[-\frac{\gamma^2}{2}(a - vt)^2\right]\right\}.$$

Here, the factor $1/a^2$ is introduced in front of the integral for the purpose of normalization. To simplify the writing, we shall introduce the dimensionless parameter $\delta = \gamma a$. In this case, the function I(t) will assume the form:

$$I(t) = \frac{B\varepsilon}{2}\left\{\left(1 + \frac{t}{\tau}\right)\Phi\left[\delta\left(1 + \frac{t}{\tau}\right)\right] - 2\frac{t}{\tau}\Phi\left(\delta\frac{t}{\tau}\right) + \right.$$
$$+ \left(1 - \frac{t}{\tau}\right)\Phi\left[\delta\left(1 - \frac{t}{\tau}\right)\right] +$$
$$+ \frac{2}{\sqrt{2\pi}} \frac{1}{\delta} \exp\left[-\frac{\delta^2}{2}\left(1 + \frac{t}{\tau}\right)^2\right] -$$

$$-\frac{4}{\sqrt{2\pi}}\frac{1}{\delta}\exp\left[-\frac{\delta^2}{2}\left(\frac{t}{\tau}\right)^2\right]+$$
$$+\frac{2}{\sqrt{2\pi}}\frac{1}{\delta}\exp\left[-\frac{\delta^2}{\delta}\left(1-\frac{t}{\tau}\right)^2\right]\Bigg\}, \quad (1)$$

where $\tau = a/v$.

One can find the signal at the output of a photodetector with a pulse response of

$$\varphi_1(t) = \beta e^{-\beta t},$$

where β is the time constant, by means of a Duhamel integral [1]:

$$\psi(t) = \int_0^t I(\theta)\,\varphi_1(t-\theta)\,d\theta. \quad (2)$$

By substituting I(θ) from (1), and taking the integral (2), we find

$$\psi(t) = \frac{B_0}{2}\left(1+\frac{t}{\tau}-\frac{1}{\beta\tau}\right)\Phi\left[\delta\left(1+\frac{t}{\tau}\right)\right]+$$
$$+\frac{B_0}{2\beta\tau}\exp\left[-\beta(t+\tau)+\frac{\beta^2\tau^2}{2\delta^2}\right]\left\{1+\Phi\left[\delta\left(1+\frac{t}{\tau}-\right.\right.\right.$$
$$\left.\left.\left.-\frac{\beta\tau}{\delta^2}\right)\right]\right\}+\frac{B_0}{\sqrt{2\pi}}\frac{1}{\delta}\exp\left[-\frac{\delta^2}{2}\left(1+\frac{t}{\tau}\right)^2\right]-$$
$$-B_0\left(\frac{t}{\tau}-\frac{1}{\beta\tau}\right)\Phi\left(\delta\frac{t}{\tau}\right)-\frac{B_0}{\beta\tau}\exp\left(-\beta\tau+\frac{\beta^2\tau^2}{2\delta^2}\right)\times$$
$$\times\left\{1+\Phi\left[\delta\left(\frac{t}{\tau}-\frac{\beta\tau}{\delta^2}\right)\right]\right\}-\frac{2B_0}{\sqrt{2\pi}}\frac{1}{\delta}\exp\left[-\frac{\delta^2}{2}\left(\frac{t}{\tau}\right)^2\right]+$$
$$+\frac{B_0}{2}\left(1-\frac{t}{\tau}+\frac{1}{\beta\tau}\right)\Phi\left[\delta\left(1-\frac{t}{\tau}\right)\right]+$$
$$+\frac{B_0}{2\beta\tau}\exp\left[-\beta(t-\tau)+\frac{\beta^2\tau^2}{2\delta^2}\right]\left\{1+\Phi\left[\delta\left(\frac{t}{\tau}-1-\right.\right.\right.$$
$$\left.\left.\left.-\frac{\beta\tau}{\delta^2}\right)\right]\right\}+\frac{B_0}{\sqrt{2\pi}}\frac{1}{\delta}\exp\left[-\frac{\delta^2}{2}\left(\frac{t}{\tau}-1\right)^2\right]. \quad (3) \quad (3)$$

The signal is fed from the output of the photodetector to the input of an amplifier, which has a finite passband Δf. We shall assume that the scanning rate is rather high, so that $f_B >> f_H$ [$f_B = f_{upper}$, $f_H = f_{lower}$] and the equivalent noise bandwidth of the amplifier $\Delta f_n \approx f_B$, i.e., the influence of photodetector noise with a spectral density of 1/f can be disregarded. Under these conditions, one can assume that the pulse response of the amplifier is:

where
$$\varphi_3(t) = \alpha e^{-\alpha t}, \quad \alpha = 2\pi f_в. \tag{4}$$

We derive the signal at the output of the amplifier by secondarily employing the Duhamel integral of thefunction (3) for the case of pulse response (4):

$$U(t) = \int_0^t \psi(\theta)\,\varphi_3(t-\theta)\,d\theta.$$

As a result of integration, we have:

$$U(t) = \frac{Bs}{2}(a_{+1} - 2a_0 + a_{-1}), \tag{5}$$

where

$$a_n = \left(\frac{t}{\tau} + n - \frac{\alpha+\beta}{\alpha\beta\tau}\right)\Phi\left[\delta\left(\frac{t}{\tau}+n\right)\right] - \frac{\alpha}{\beta\tau}\frac{1}{\beta-\alpha}\exp\left[-\beta(t+n\tau) + \frac{\beta^2\tau^2}{2\delta^2}\right]\left\{1+\Phi\left[\delta\left(\frac{t}{\tau}+n-\frac{\beta\tau}{\delta^2}\right)\right]\right\} + \frac{2}{\sqrt{2\pi}}\frac{1}{\delta}\exp\left[-\frac{\delta^2}{2}\left(\frac{t}{\tau}+n\right)^2\right] + \frac{\beta}{\alpha\tau}\frac{1}{\beta-\alpha}\exp\left[-\alpha(t+n\tau) + \frac{\alpha^2\tau^2}{2\delta^2}\right]\times\left\{1+\Phi\left[\delta\left(\frac{t}{\tau}+n-\frac{\alpha\tau}{\delta^2}\right)\right]\right\}.$$

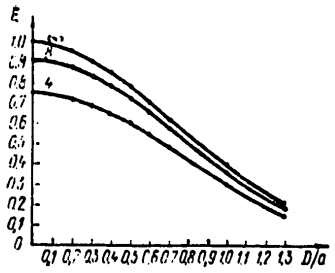

Figure 1. The quantity ξ as a function of the circle of confusion D. The numbers on the curves correspond to the values of βτ

Expression (5) defines the signal when scanning one strip in the field of the objectives. To obtain the signal which appears when two strips are scanned, based on our hypothesis, which are located in the field of the objectives, it is necessary to add to the signal defined by function (5) the same signal shifted in time by the amount 2τ:

$$U_{out}(t) = U(t) + U(t-2\tau). \tag{6}$$

The output signal corresponding to the following values of the diameter of the circle of confuction D, defined with respect to the 0.5 level was computed on a "Minsk-32" computer using formulas (5) and (6) when B = 1 and ε = 1: 0, 0.2a, 0.3a, 0.4a, 0.5a, 0.6a, o.7a, 1.0a and 1.3a for a set of values of ατ ranging in an

interval from 3 to 12 with a step of 0.05, and for $\beta\tau = 2$, 4, 8 and ∞. The resulting curves have two maxima and minima between them. We shall designate the value of the function at the first maximum U_1 and at the minimum U_2, and U_3 at the second maximum. Based on these extremal values of the function, the sizes of the relative dip in the curves were computed:

$$g = \frac{\frac{U_1 + U_3}{2} - U_2}{\frac{U_1 + U_3}{2}}$$

$$\xi = \frac{U_1 + U_3 - 2U_2}{2\sqrt{\alpha\tau}} = g\mu, \qquad (7)$$

where the quantity $\mu = \frac{U_1 + U_3}{2\sqrt{\alpha\tau}}$ is proportional to the ratio of the average value of the signal to the mean square value of the noise. As follows from expression (7), the quantity ξ, which is proportional to the ratio of the value of the dip to the mean square value of the noise, can serve as a characteristic for the optimality of the optical-electronics system.

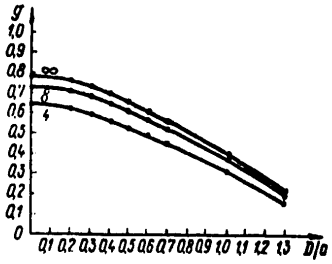

Figure 2. The relative dip g as a function of the diameter of the circle of confusion D. The numbers on the curves correspond to the values of $\beta\tau$.

Shown in Figure 1 is ξ as a function of the diameter of the circle of confusion for various values of the time constant of the photodetector; the plotted curves correspond to the optimum choice of the passband of the amplifier, i.e., to that value of $\alpha\tau$, which provides for a maximum of ξ.

Similar curves are shown for the quantity g in Figure 2. The calculation demonstrated that the optimum value of $\alpha\tau$ practically does not depend on the diameter of the circle of confusion, and is approximately equal to 3.75. It follows from this that the value of the signal waveform factor, K_{wf}, in the formula for calculating the upper boundary frequency [2] is:

$$f_B = f_{upper} = K_{wf}/\tau, \text{ and,}$$

is equal to 0.6.

The curves shown in Figures 1 and 2 can serve as the basis for quantitative estimates of the power and angular resolving powers of a thermal viewer when the circle of confusion of the optical system varies within broad limits.

BIBLIOGRAPHY

1. Shestov N.S., "Vydeleniye opticheskikh signalov na fone sluchaynykh pomekh" ["The Discrimination of Optical Signals Against a Background of Random Interference"], Moscow, Sovetskoye Radio Publishers, 1967.

2. Karizhenskiy Ye.Ya., Miroshnikov M.M., OMP [OPTICAL-MECHANICAL INDUSTRY], 1970, No 9, p 39.

8225
CSO: 8144/976

PHYSICS

UDC 620.179.18:681.786

AN ANALYSIS OF THE METROLOGICAL CAPABILITY OF A COHERENT OPTICAL METHOD OF MONITORING THE SHAPE OF COMPLEX SURFACES

Leningrad OPTIKO-MEKHANICHESKAYA PROMYSHLENNOST' in Russian No 11, 1978 pp 8-10

[Article by V.A. Kudryavtsev, V.S. Shapov and candidate in the engineering sciences V.I. Shanin, manuscript received 17 Feb, 1978]

[Text] An estimate is given for the metrological capabilities of an optical method of monitoring the shape of complex surfaces, based on the spatial coding of information and optical filtration. The dependence of the maximum of the correlation response on the change in the radius of the surface and the parameters of the encoding grating is demonstrated. The requirements placed on the orientation of products during the testing are determined.

An optical procedure for automatically monitoring the shape of complex surfaces, based on spatial encoding of the information and optical matched filtration was studied in the literature [1 - 3]. Its physical principles, specific features and areas of application were discussed, and recommendations were also given as regards the selection and topology of the elements in the structural configuration of the monitor system.

This article is devoted to a theoretical analysis of the metrological capabilities of the method and the determination of the requirements placed on the orientation of the products at the monitor position.

In accordance with the algorithm adopted for information processing, the characteristic of the surface being monitored (suitable or reject) is given based on the magnitude of the correlation response of the quality control system, which is mathematically described by the expression:

$$K_{1,2}(Q) = |t_1(x, y; Q) * t_2(x, y; Q + \Delta Q)|^2, \quad (1) \tag{1}$$

where Q is a variable parameter which characterizes the state of the surface being checked; x and y are the coordinates of the filtration

plane; t_1 is the amplitude transmittance of the transparency with the image of the reference standard surface; t_2 is the amplitude transmittance of the transparency with the image of the surface being monitored; * is the sign for a correlation operation.

Thus, to calculate the correlation response as a function of the change in the shape of the surface and its orientation with respect to the original position, it is necessary to know the amplitude transmittance $t(x, y)$, the synthesis of which in the procedure proposed here is accomplished using the configuration shown in Figure 1. The collimated light flux of source 1, which is produced by optical system 2, passes through the encoding grating 3 and falls on the surface of the product being monitored 4. As a result, a pattern is observed on the surface, the shape of which is uniquely related to the curvature of the surface and the viewing angle α, formed by the illumination and observation axes. Objective 5 forms the image of the surface being checked in its rear focal plane. It is represented on transparency 6 which is fed to the input of the information processing channel.

The structure of the image on the transparency is determined by three factors: the encoding grating, the condition of the surface and the viewing angle. When checking a batch of identical products, the parameters of the encoding grating and the viewing angle are constant, and consequently, the structure of the image depends entirely on the condition of the surface.

The research which has been carried out in this direction has made it possible to establish the fact that the images of such surfaces, such as cylindrical, conical, spherical and all possible combinations of them, when illuminated through an encoding grating in the form of a system of alternating transparent and opaque lines, take the form of a set of bands of an elliptical type.

Taking into account what has been presented here, as well as the fact that the majority of products produced by industry consists of surfaces of the types enumerated above, we shall limit ourselves to a treatment of the case of the quality control of products with a cylindrical surface. We shall perform the calculations only for the maximum of the correlation response, something which corresponds to the physical conditions for estimating it.

Let the product be positioned so that the direction of illumination is perpendicular to its surface and the generatrix of the surface is parellel to the horizontal plane. If the radius of the cylindrical surface is called R, and the width of a line in the encoding grating is a, then the transmittance of the transparency for one line in the surface image can be written as follows:

$$t(x, y) = \begin{cases} 1 \text{ при } |y| < R;\ \sqrt{R^2 - y^2}\sin\alpha + \\ \quad + a\cos\alpha > x > \sqrt{R^2 - y^2}\sin\alpha, \\ 0 \text{ в остальной области.} \end{cases} \qquad (2)$$

[0 in the remaining region]

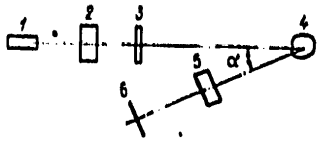

Figure 1. The configuration for synthesis of the transparencies.

Such a formulation for the transmittance presupposes 100 percent modulation of the recording medium of the transparency, something which is assured by the suitable selection of the exposure time and the way it is processed.

Following the substitution of (2) in (1), integration and normalization, we obtain the following expression for the determination of the maximum of the correlation response:

$$K_{\max}(m, A) = \begin{cases} \left[m + \frac{m(1-m)}{A} + \frac{\pi m^2}{4A} - \right. \\ \left. - \frac{m\sqrt{1-m^2}}{2A} + \frac{\arcsin(m)}{2A}\right]^2 \quad (3.1) \\ \text{при } A > m - 1 + \sqrt{1-m^2},\ m < 1; \\ \left[\frac{m^2}{2A}\left\{\arccos\left(\frac{b-c}{m}\right) - \right.\right. \\ \left. - \left(\frac{b-c}{m}\right)\sqrt{1-\left(\frac{b-c}{m}\right)^2}\right\} + \\ + \frac{1}{2A}\left\{(b+c)\sqrt{1-(b+c)^2} - \right. \\ \left.\left. - \arccos(b+c)\right\}\right]^2 \quad (3.2) \\ \text{при } A < m - 1 + \sqrt{1-m^2},\ m < 1; \\ \left[1 - \left\{\frac{m^2}{2A}\arcsin\left(\frac{1}{m}\right) - \frac{\pi}{4A} + \right.\right. \\ \left.\left. + \frac{\sqrt{m^2-1}}{2A} - \frac{m-1}{A}\right\}\right]^2 \quad (3.3) \\ \text{при } A > 1 - m + \sqrt{m^2-1},\ m > 1; \\ \left[\frac{1}{2A}(\arccos f - f\sqrt{1-f^2}) + \right. \\ \left. + \frac{m^2}{2A}(\arccos q - q\sqrt{1-q^2})\right]^2 \\ \text{при } A < 1 - m + \sqrt{m^2-1},\ m > 1, \quad (3.4) \end{cases}$$

where

$$m = h/l_{\max};\ A = \frac{a}{R}\operatorname{ctg}\alpha;\ b = \frac{1-m^2}{2(1+A-m)};$$

$$c = \frac{1+A-m}{2};$$

$$f = \frac{2m-2+A^2}{2(m+A-1)} - A;\ q = \frac{2m-2+A^2}{2m(m+A-1)} + \frac{m-1}{m};$$

R_0 is the radius of the reference standard surface, and $0° < \alpha < 90°$.

Formulas (3.1) and (3.2) correspond to the case of monitoring a surface with a radius less than the reference standard one, while (3.3) and (3.4) correspond to the case where the radius is greater than the reference standard one. Curves for $K_H(m)$ are shown in Figure 2 for three different values of the parameter A and a viewing angle of $\alpha = 45°$. The family of curves to the left of the ordinate corresponds to $m < 1$, and those to the right, to $m > 1$. It can be seen from the graphs that the sensitivity of the method to the ascertaining of deviations in the shape of the surface being tested from the reference standard surface increases with a decrease in the line width a in the encoding grating. A quantitative analysis of expression (3), taking into account the actual characteristics of objectives which are produced, demonstrated that the relative sensitivity, defined as the ratio of the amount of the deviation ΔR to the size of the requisite radius, R, is on the order of 10^{-3} -- 10^{-4}. Its maximum value is achieved when:

$$a = 10\frac{R}{D}P$$

where D is the size of the objective aperture in the information processing channel; P is its resolving power.

The nature of the sensitivity ($\Delta R/R$) as a function of the parameter A for several threshold levels of K_H of practical interest is illustrated in Figure 3.

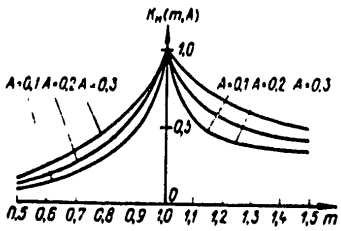

Figure 2. The maximum of the correlation response as a function of the variation in the radius of the surface being monitored.

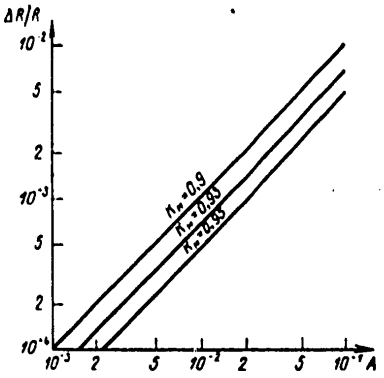

Figure 3. The sensitivity $\Delta R/R$ as a function of the parameter A.

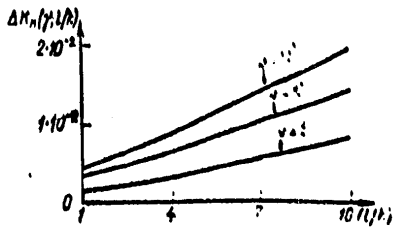

Figure 4. The amount of the reduction in the maximum of the correlation response as a function of the orientation of the product in a transverse plane.

Moving on to the classes of precision in the machining of surfaces which are in force in the system of the industrial sector standard, it is not difficult to come to the conclusion that the method developed here permits the monitoring of products manufactured in accordance with the second class of precision.

It was presumed up to now that the positions of the monitored and calibration reference products coincide. Under actual conditions, though, by virtue of destabilizing factors, mismatching is to be anticipated between the positions of the products. We shall consider its influence on the magnitude of the correlation response maximum.

It is well known from the theory of optical matched filtration [4] that the magnitude of the correlation response falls off when the angular orientation of the image being analyzed does not agree with that of the reference standard (in the horizontal and vertical planes). In our case, a rotation of the product in the horizontal plane is equivalent to a change in the viewing angle α. It is not difficult from expression (3) to find the relative reduction in the correlation response maximum, which will be equal to:

$$\Delta K_{\max}(\Delta\alpha) = \left| 1 - \frac{\operatorname{tg}^2(\alpha \pm \Delta\alpha)}{\operatorname{tg}^2(\alpha)} \right|.$$

An analysis of the resulting function shows that a deviation of the product from the requisite position by 10 -- 15' leads to a reduction in the correlation response maximum by 1%, i.e. to a change in it by an amount which cannot be reliably recorded because of the instability and fluctuating noise of the photodetector [5]. Providing for the precision indicated here in the orientation of the products at the test position presents no difficulties using existing equipment.

To determine the requirements placed on the orientation of products in the transverse plane, we shall make use of the fact [4] that the correlation response of the optical devices for matched filtration, when the angular position of the image being analyzed changes, depends on it configuration. In this case, the greatest criticality is observed when analyzing images with a contour in the form of straight lines. For this reason, we estimated the influence of the precision in the setting of the product in the transverse plane on the correlation response using the example of the product in the

form of a rectangle. The transmittance of the transparency in this case has the form:

$$t(x, y) = \mathrm{rect}(x/l)\,\mathrm{rect}(y/h), \tag{4}$$

where

$$\mathrm{rect}(z) = \begin{cases} 1 \text{ при } |z| < 1/2 \\ 0 \text{ в остальной области;} \end{cases}$$

h is the width of the rectangle and l is its length.

After substituting (4) in (1), integration and normalization, we derive the expression for the calculation of the correlation response maximum:

$$K_{\text{н}}(\gamma;\, l, h) = \left[1 - \left\{\left(\frac{l^2 + h^2}{4lh}\right)[1 + \mathrm{tg}^2(\gamma/2)] - \mathrm{tg}(\gamma/2)\right\}\mathrm{tg}(\gamma)\right]^2,$$

where γ is the angle of rotation of the product in the transverse plane.

Shown in Figure 4 are the amounts of reduction in the correlation response maximum as a function of a geometric factor (l/h) for three values of the angle γ. It can be seen from a comparison of the curves that in the case of a geometric factor ≤ 5, a reduction in the correlation response maximum by 1% is achieved with a deviation of the product from the requisite position 10--15', which, as has already been noted, can be assured.

Conclusions

1. An optical procedure for automatically monitoring the shape of complex surfaces has a relative sensitivity on the order of 10^{-3}--10^{-4}, i.e., allows for the quality control of products belonging to the second class of precision.

2. The deviation of a product when it is oriented in a test position from the requisite position by 10--15' has practically no effect on the quality of the test operation; it is not difficult to assure such precision in the orientation of the product.

BIBLIOGRAPHY

1. Mirovitskiy D.I., Samsonov G.A., Shanin V.I., RADIOTEKHNIKA I ELEKTRONIKA, 1972, Vol 17, No 6, pp 1280 - 1285.

2. Will P.M., Pennington K.S., PROC. IEEE, 1972, No 6, p 22-36.

3. Van der Lugt A., IEEE TRANS., 1964, Vol 2, p 139-145.

4. Van der Lugt, et al., ZARUBEZHNAYA RADIOELEKTRONIKA [FOREIGN RADIO ELECTRONICS], 1968, No 3, pp 53-67.

5. Kovalevskiy V.A., "Metody optimal'nykh resheniy v raspoznavanii izobrazheniy" ["Optimum Solution Methods in Image Recognition"], Moscow, Nauka Publishers, 1976.

8225
CSO: 8144/976

PHYSICS

UDC 663.3:666.22:542.68

RESULTS AND DEVELOPMENTAL PROSPECTS IN OPTICAL CERAMICS

Leningrad OPTIKO-MEKHANICHESKAYA PROMYSHLENNOST' in Russian No 11, 1978
pp 39-41

[Article by candidate in the sciences, F.K. Volynets, manuscript received 12 April, 1978]

[Text] The main optical, physical and chemical characteristics of optical ceramics, obtained by the method of gas pressing are given. Its most promising areas of application are indicated.

The birth of optical ceramics - the polycrystalline class of optical materials - was due to the developmental needs of optical science and engineering, and in particular, to the widescale introduction of thermal viewing into the national economy which started at the beginning of the 1950's. Optical materials were required in this regard which have a high mechanical strength and good transparency in the IR region of the spectrum. Classical optical materials, silicate glasses and monocrystals, did not possess the indicated combination of properties. The former, though having good structural characteristics, as is well known, are opaque in the region of the spectrum above 3.5 μm, while the latter, on the other hand, while having good transparency in the IR region are mechanically anisotropic, and for this reason, as a rule, are not structural materials. In this regard, the development of polycrystalline optical materials proved to be necessary, since only they could combine isotropicity of mechanical properties with high transparency in the IR range of the spectrum. Such an assessment and prognosis were confirmed by three factors:

1) Nature has created a number of polycrystalline silicate minerals, which are distinguished by exceptionally high mechanical strength (nephrite, agate, etc.);

2) Spectroscopists have developed the so-called KBr method of studying the absorption spectra of various materials by pressing them into potassium bromide;

3) The development of ceramic technology led to the creation of a production technology at the end of the 1940's for a very dense tool ceramic.

In this way the problem was reduced to the development of fabrication technology procedures for polycrystalline materials, which possessed the following:

a) A porosity one to two orders of magnitude lower than that of tool ceramic (0.3--0.03 vol.%, instead of 3--5%), because of which they become transparent in the optical and even in the visible range of electromagnetic radiation;

b) Considerably greater strength than tablets of KBr;

c) Transparency in various IR spectral ranges, right up to 30--50 μm.

This condition necessitated the applicability of the procedure being worked out for the fabrication of polycrystalline optical materials from substances belonging to various classes of chemical compounds: oxides, fluorides, chalcogenides.

We started work on the creation of ceramics in 1959. Samples of various materials were obtained during 1961--1967. However, intense developmental work on the physical and chemical fundamentals of the production technology for optical ceramics and all of their components (raw materials, production equipment, ways of producing blanks of the requisite dimensions, shapes and quality) were started in 1968.

The so-called "hot pressing" method for a dispersed powder was taken as the basis for the solution of the problem. The factors governing the choice were as follows: in the first place, this procedure is distinguished by its universality and provides for obtaining optical ceramics from various substances, including those from low temperature variants in some cases, and secondly, low relative pressing temperatures (≈ 0.66 [T, fusion]) open up the possibility of deriving blanks with a fine crystalline structure, without turning to the introduction of additives which inhibit secondary recrystallization. A reduction in the average size of the grain is important from the standpoint of increasing mechanical strength, heat resistance, as well as reducing light scattering in the case where ceramics are fabricated from optically anisotropic materials and the electro-optical characteristics of optical feroelectric ceramics; thirdly, the method is distinguished by its economy: the simultaneous action of temperature and pressure permits not only a substantial in the compaction temperature, but also approximately a doubling of the compaction rate. In this case, the derivation of the material and the blanks in simple shapes are combined in one operation. The fact that the blanks were characterized by a very small ratio of height to diameter (1:10) promoted the selection of this production technology procedure.

The kinetics of the compaction of both monophase dispersed powders and powders alloyed with different additives was studied in particular. The investigations were carried out using three different schemes:

1) The degree of compaction ρ is a function of the temperature t° for a constant heating rate dt°/dt and a constant pressure p:

$$\rho = f(t^\circ)_{\frac{dt^\circ}{dt}, p};$$

2) The degree of compaction is a function of the pressure for the case of a constant deformation rate $\varepsilon = d\varepsilon/dt$ and a constant temperature:

$$\rho = f(p)_{\frac{d\varepsilon}{dt}, t};$$

3) The degree of compaction is a function of time with a constant temperature and pressure: $\rho = f(t)_{t^\circ, p}$.

The studies of the compaction kinetics using these schemes were necessary in the theoretical plan to establish the operative elementary mechanisms of the mass transfer; and along with this, they were analogs of the basic stages of the technological process: cold pressing, heating, the application of pressure and maintainance under pressure at the pressing temperature. These studies were carried out using both specially designed dilatometric installations and an all-purpose test machine. The structure of the samples obtained, the kinetics of secondary recrystallization, the texture formation mechanism, the dependence of microhardness and transparency on the pressing conditions, and in some cases, the temperature dependence of the ultimate strength and yield limit, as well as the radial gradients of the density and texture in the blanks, were all studied simultaneously using the methods of density measurement, spectrophotometry, optical interferometry in white and polarized light, as well as X-ray structural analysis and optical polarization analysis.

The studies were carried out using samples of materials of interest for optical science and engineering, and additionally, which differed substantially in the type of chemical bond, the structure of the crystal lattice, and which also belonged to different classes of chemical compounds: MgF_2, MgO, ZnS, ZnSe, CdS, CdTe, BaF_2, CaF_2, $PbCl_2$, PbI_2, CsI, Y_2O_3, La_2S_3, etc. The powders which were studied differed by more than two orders of magnitude as regards the degree of fineness (the average grain size fluctuated from 0.1 to 10.0 μm and more).

The studies were conducted in a broad range of thermodynamic parameters: temperatures up to 1,400° C, pressures up to 5.0 t/cm^2, exposure times of up to 180 minutes and a residual pressure down to 10^{-4} mm Hg.

A decision in favor of the vacuum pressing variant was made right at the outset of the work for the following reasons. The presence of air in the pores retards the compaction of the briquette and induces selective absorption bands due to the interaction of the material with the moisture and oxygen in the air. Moreover, the presence of gases at high pressure in the pores of the resulting optical ceramic reduces its mechanical strength, something which is especially pronounced when the temperature increases, and along with this, complicates the process of cooling the blank and its subsequent annealing. Pressing in a vacuum permits obtaining an optical ceramic from materials which oxidize easily in an air atmosphere, as well as the use of easily oxydizable heat resistant molybdenum alloys for the fabrication of the components of compression molds.

The extensive experimental material made it possible to establish the fact that the basic elemenary mechanism of mass transfer during the action of a relaive temperature of 0.5--0.8 T_{fus} and a pressure of 1.0--3.0 t/cm^2 are slip along the crystallographic planes (translational and twinning), and slip along the boundaries of the grains, as well as the ascertaining of the exceptionally important role played by the secondary recrystallization processes in attaining a relative density of the briquette of more than 0.99. The secondary recrystallization activates slip along grain boundaries, and when a certain temperature is reached, causes the transition of the briquette to a state of superplasticity. The degree of intensity of secondary recrystallization which provides for attaining a level of compaction practically equal to the theoretical level, over an exposure time of 30--60 minutes under a pressure of ≈2.0 t/cm^2 has been quantitatively determined. It consists in an increase in the average grain size of three to five times. Pressing at temperatures which provide for meeting this condition is equivalent to pressing during phase transformations. In fact, the entire volume of the briquette is subjected to recrystallization in this case.

The important part played by recrystallization processes is also determined by a number of other factors. In the first place, the relationship of the velocities of grain boundary migration and the movement of a pore located at the grain boundary determines the probability of pore capture by the growing grains. Along with an increase in the probability of pore capture, the level of compaction and the transparency of the ceramic are reduced. Secondly, secondary recrystallization produces the structure of the ceramic, and along with this, also a number of its properties. The mechanical strength of a polycrystal is related primarily to grain size. When deriving optical ceramics from anisotropic substances, grain size determines the position of the shortwave boundary of ceramic transparency, and in connection with the fact that when the grain size approaches the wavelength of the light passing through, its losses increase sharply due to scattering. Inhibiting secondary recrystallization in these cases by means of changing the pressing conditions or introducing special additives permits a substantial increase in the transparency of ceramics in the shortwave region of the spectrum.

And finally, there is yet one more governing law which underscores the exceptional part played by the secondary recrystallization processes when fabricating optical ceramics: performing the pressing with the indicated intensity of secondary recrystallization makes it equivalent to the process of growing monocrystals. The difference consists in the fact that in the case of pressing, the specific crystallization surface is quite large (≈1--10 m^2/g), where this crystallization occurs at low temperatures (≈2/3 T_{fus},°K) of the material being pressed and at very high pressures (≈2.0 t/cm^2). Establishing this governing law pointed out the possibility of obtaining luminescent optical ceramics, alloyed with those additives which cannot be introduced into a crystal lattice when growing crystals from a melt.

The facts adduced above allow us to call the pressing process under the conditions indicated here "recrystallization pressing." Such a designation unambiguously defines the nature of the physical and chemical processes which provide for attaining the theoretical density, as well as the conditions for its realization. The establishing of the governing laws considered here permit the determination of the parameters of the pressing process, by working from the physical and chemical parameters of the powder. In particular, decreasing the average grain size in the initial powder from 10 to 0.1 μm makes it possible to reduce the relative pressing temperature from 0.75--0.8 down to 0.55--0.6 T_{fus} °K, or by 200--500° on the Kelvin scale.

Moreover, it also became possible to formulate the technical specifictions for the original powders, in which their suitability for the fabrication of an optical ceramic is determined not by a technological sample test, but by their physical and chemical parameters, which, in turn, derive from the requisite microstructure of the ceramic being obtained and the capabilities of the production equipment. Along with this, the capability of fabricating an optical ceramic from any optically isotropic or weakly anisotropic material was placed on a solid footing. The justification for this position is confirmed by the photograph of samples of optical ceramics, which is shown in the figure.

Simultaneously with the working out of the physical and chemical principles of the fabrication technology for optical ceramics, a procedure was created for synthesizing the starting materials and equipment, which permitted as early as 1968 undertaking the development of a production process for the fabrication of the requisite blanks of optical ceramics based on magnesium fluoride. A number of production processes were worked out which provide for obtaining blanks in the smplest shapes with a diameter of up to 350 mm at pressing temperatures up to 1,200° C. Series production of optical ceramics has been organized on the basis of these blanks.

Searches for heat resistant structural materials based on molybdenum, which assure operability of compression molds at temperatures up to 1,500° C and pressures up to 2.5 t/cm^2 were undertaken in the past decade in conjunction with institutes engaged in the development of metals. This circumstance will

produce a completely new situation in the plan for the development and application of optical ceramics. A decisive factor in their development is not the capabilities of the production equipment, but rather the vital needs of optical science and engineering. In this case, in accordance with the mutual conditionality of the phenomena, such broad, essentially unlimited experimental capabilities in the design of optical ceramics with new optical, physical, chemical and operational properties, or new combinations of them, in turn permit optical ceramics participating to a more marked degree in accelerating the development of optical scinece and engineering. It is well known that the products list and the quality of optical materials will serve as one of the indicators of the level of the nation's optical science and engineering.

Of course, it does not follow from this that the technological production procedures for the fabrication of blanks of optical components using the method of recrystallization pressing, both one-sided and isostatic pressing are not subject to refinement for the purpose of reducing the manufacturing labor intensity and increasing their quality. One of the most urgent tasks is the automation of the production process. It is becoming economically justified and necessary in connection with the large series production of blanks of optical ceramics. This is an extraordinarily complex problem. However, it should be noted that several of the physical and chemical prerequisites for its solution have already been found.

Extensive and systematic research into the physical, physical chemistry and operational characteristics of optical ceramics has been undertaken simultaneously with their development and introduction into production.

The study of properties of optical ceramics has not only promoted an expansion of the applications areas and an acceleration of the rates of introduction of optical ceramics as an optical structural material, but has also made it possible to ascertain the effectiveness of their application in other fields of optical engineering. We should primarily point out the construction of objective lenses. Chalcogenide and certain optical oxide ceramics are the most promising, which possess a refractive index equal to or greater than 2.0, as well as fluoride ceramics, which permit compensating for their chromatic aberration. Because of the monophase aspect (single component aspect) of optical ceramics, they are characterized by a rather high optical homogeneity ($\Delta n = 10^{-3}$--10^{-5} at a wavelength of 1 μm), which completely permits their application in lens systems. This is also being promoted by the success achieved in recent years in increasing the transparency of optical ceramics in the visible region of the spectrum, which permits not only the visual adjustment of instruments, but also their operation in this region of the spectrum. The index of absorption of optical ceramics amounts to

$\approx 10^{-1}$ cm^{-1}. However, there is a basis for obtaining optical ceramics with an index of absorption one to two orders of magnitude lower. The solution of this problem will permit the wide utilization of optical ceramics in gas laser engineering, and expand the possibility for their application in the construction of objectives.

An important factor which promotes the introduction of optical ceramics in the construction of objectives would be the development of a production process for the manufacture of blanks with even one surface, including an aspherical surface, which does not require additional cold working machining. The theoretical possibility of solving this problem has been confirmed for a long time by individual experiments, but there is as yet no technological process. Such a situation is explained by the complexity of the problem, and it can be said, its elegance, which requires knowledge of the quantitative relationships between the shape generating surfaces of the compression mold and the resulting blank, which are due to the relationship between the modulus of elasticity, the coefficient of thermal expansion and the coefficients of heat conductivity of the material of the compression mold and the ceramic being fabricated. Moreover, the deserved attention has not been devoted to the solution of this problem, although it promises a considerable technical and economic effect.

Also promising is the application of optical ceramics in spectral instrument construction as the windows of cells, the substrates of absorption and interference light filters, reflective light filters, etc., especially in a spectral range of 12--25 μm.

The study of the physical and chemical nature of the processes involved in the fabrication of optical ceramics by the method of recrystallization pressing has indicated the possibility of obtaining luminescent optical ceramics. These ceramics are promising for devices which visualize radiation: neutron, electron, X-ray, ultraviolet and infrared radiation. Such an assessment is due to two arguments. On one hand, optical ceramics, in contrast to luminescent glasses and monocrystals, possesses a high luminescence light yield, which is comparable to the light yield of powder luminophors (2--10 candles/W). On the other hand, it is just as strong as glass and monocrystals, and combines the better qualities of all of the well known luminescent materials. Along with this, the technological process of recrystallization pressing provides for the capability of fabricating a luminescent optical ceramic from practically all of the well well known powder luminophors.

Considerable effectiveness is anticipated from the introduction of electro-optical ceramics into optical information processing equipment as the working medium for high speed multichannel modulators and page generators for holographic systems. The use of electro-optical ceramics will make it possible to boost the operational speed by three to four orders of magnitude as compared to liquid crystal cells. The promise of magneto-optical ceramics should likewise be noted. Experience has demonstrated the effectiveness of

the application of optical ceramics in the solution of a number of special problems (the input windows of radiation receivers, directional radiation scatterers, high intensity plasma light sources, coating optics, etc.). The promising outlook for the application of optical ceramics in various science and engineering, which were discussed here, allow for the conclusion that the class of polycrystalline optical materials has just begun its period of intensive development.

8225
CSO: 8144/976

PHYSICS

UDC 535.313.2

THE BASIC PRINCIPLES OF THE AUTOMATION OF THE PROCESS OF SHAPING ASTRONOMICAL OPTICS

Leningrad OPTIKO-MEKHANICHESKAYA PROMYSHLENNOST' in Russian No 11, 1978 pp 42-45

[Article by Academician A.M. Prokhorov, and candidates in the sciences Ye.V. Trushin and E.A. Vitrichenko]

[Text] Possible methods of controlling the process of shaping optical surfaces with the use of computers are analyzed. It is shown that an efficient way of automating the shaping process is real time program control of the local pressure of a small tool on the component.

A whole series of difficulties arise in the fabrication of astronomical optics with large dimensions. These difficulties are primarily related to the fact that it is necessary to maintain a certain mathematical surface within a precision of a few hundredths of a micrometer on a large optical surface area, figured in square meters.

The solution of the problem is impeded, for example, by the following factors. In the first case, nonuniformity of the hardness over the surface of the blank itself leads to a differing degree of removal of the material with equal machining conditions. In the second place, the imperfection of the optical machine tool, as well as effects of its alignment lead to various types of errors in the optical surface. Thirdly, temperature effects related to inhomogeneous heating of the component and the tool in the machining process also lead to errors. Fourthly, nonuniformity in feeding the polishing suspension to the point of contact of the optical component with the tool also has an effect. Fifthly, the imperfection of the tool and its wear cause additional errors [13].

The existing practice of optical manufacturers is based on experience and intuition, and not on precise data concerning the technological process. Such practive leads to the fact that the process of fabricating the optical surfaces is not a convergent one, i.e., in the process of working on a component, the practicing optical worker improves the quality of the components

some of the time, but part of the time is involuntarily spent degrading it. For this reason, outlays for the fabrication of large optical surfaces prove to be unjustifiably high.

With the operational method adopted, the quality of the finished optical product depends on the skill of the experienced optical worker. This introduces a subjective factor into optical technology. For example, one optical worker "can" manufacture a certain component with high quality, while another will not achieve this quality in any amount of machinging time.

A way out of the situation which has developed can be the automation of the shaping process using computer equipment. In this case, the technological process will become a strictly convergent one, i.e., in each processing session, the optical surface will only be improved, and moreover, the process would become independent of the personal experience of the experienced optical worker.

It would be extremely tempting to design a fully automated installation for the fabrication of optical surfaces. In this case, checking the shape of the surface and the shaping process itself (grinding or polishing) should be accomplished in real time. Unfortunately, not only is monitoring of the shape of the surface during its processing not realized at the present time, but there are not even any ideas of how to do this in the immediate future. For this reason, the process can be done only in an automated manner, but not automatically.

The most important guarantee of success in fabricating an optical surface is operationally timely quantative monitoring of its shape, as well as the linking of this monitoring to the technological process. This question is not discussed in this article. Since quantitative checking of ground surfaces is just now being developed [24], it is more convenient to begin the automation with the polishing stage, where the methods of checking are rather well worked out.

The rapid development of digital engineering has opened up new possibilities for optical technology. It is well known that the application of computers has caused a revolution in mathematical optics [6]. Digital and analog electronic equipment has exerted a considerable influence on the procedures for studying optical components and systems. In particular, the processing of measurements using the Hartman method is carried out with a computer [2, 22, 25 - 27], and work has begun on the automation of Hartman photograph measurements [28]. Analog equipment is used for the quantitative shadow Foucault-Filbert method [11, 19, 23]. Digital and analog equipment is used in the interferometric testing of optical components [17, 18].

The first steps have also been taken in the field of the application of digital engineering to the automation of the shaping process [14, 16, 29].

Possible Ways of Automating the Shaping Process

In accordance with a hypothesis of Preston [20, 21], the justification for which has been repeatedly verified [5, 16], the following relationship is observed in the process of machining an optical surface (grinding or polishing) for each of its elements:

$$dh = K(a_1, a_2, a_3)\, pvdt, \tag{1}$$

where dh is the amount of material removed; dt is the elemental machining time; p is the specific pressure of tool on the component; v is the velocity of the tool with respect to the component, K is atechnological constant which depends on the component material a_1, the tool material a_2 and the properties of the abrasive material a_3.

An elementary analysis of formula (1) shows that in principle, we can control four technological functions:

--The machining time for each elemental area;

--The velocity of the tool with respect to the component;

--The trajectory of the tool on the optical surface;

--The pressure (force) of the tool on the component.

A combination control procedure is also possible.

It is difficult to control the first three functions independently of the influence of the other functions. In this sense, the breakdown in control methods discussed in the following (with the exception of pressure control) is conditional.

Control of the local pressure of the tool on the component does not depend on the remaining technological parameters. This is the most important merit of the method.

Control of the Machining Time

We shall consider two methods of controlling the machining time: direct control and the mask method. These methods can also be considered control of the tool trajectory.

Direct control of the machining time was realized in the following manner [10]. Three small tools were positioned on guides, making an angle of 120°. The component (a plane mirror 1 meter in diameter) was broken down into annular zones with a width of 0.1 m, and the machining time for each

zone was computed from the formula of [1]. The tool pressure was constant, and the change in velocity was taken into account.

The advantages of the method are the simplicity of the realization and the possibility of total automation. There are two drawbacks to this procedure. In the first case, it is impossible with this method to eliminate local errors; moreover, it is well known that for astronomical mirrors, it is specifically this type of error which is characteristic [3]. Secondly, because of the discrete nature of the machining, there is an edge effect, i.e., zonal errors arise, the size of which are approximately equal to the size of the zones into which the component is subdivided.

The mask method, worked out by the Tsesnek group [9] was based on the use of a full-size tool, the working surface of which was made in the form of lobes. The shape of the lobes was computed so as to provide the requisite removal of material.

A merit of the mask method is the abscence of edge effects inherent in methods in which a small tool is used. Included among the drawbacks are the complexity of realizing the method, which is related to the necessity of fabricating a special tool for each machining session, and the fundamental impossibility of eliminating non-axial symmetric errors.

Controlling the Tool Speed

The velocity of the tool with respect to the component has three components: the rotational velocity of the component, the rotational velocity of the tool and the velocity related to the motion of the carrier. Because of the large amount of system inertia, control of the velocities is difficult for astronomical mirrors, but in machine tools of the"Start" type, velocity control has been realized for the upper link using a small tool.

In a number of foreign patents [14, 15], methods of velocity control of the component have been described, but these methods are hardly applicable to large products.

Controlling the Trajectory of the Tool

This method was realized by the American company "Itek" [15, 16]. A trajectory which provided for the requisite removal of material was realized using a specially designed machine tool, which permitted arbitrarily moving the small tool in two mutually perpendicular directions. The trajectory is calculated beforehand on a computer. The method was successfully tested in the fabrication of mirrors with a diameter of about a meter. Over several hours of finishing, a surface quality was successfully achieved with a mean square error of $\lambda/40$, something which satisfies Marechal's condition [30].

The control procedure realized by the "Itek" company can be applied to the method of machining time control, since the trajectory is figured by working from the proportionality between the exposure time and the requisite level of removal.

An article by associates of another American company, "Perkin-Elmer", appeared not long ago [29], which describes an even more refined technological system, including a computer.

The major merit of the systems indicated here is the possibility of eliminating local errors and fabricating components with a complex shape, for example, off-axis paraboloids. The single drawback is the necessity of a special machine tool.

The fabrication of such a machine tool, as well as a special tool for the mirror is a necessary condition for the realization of all control methods described above, something which substantially complicates the application of these methods in industry, since two difficulties arise here: the first of them is of an economic nature and is related to the necessity of replacing the set of machine tools, something which leads to large outlays of time and equipment. The second is of a psychological nature, and to overcome it can prove to be even more complex. Optical machine tools have changed little over recent decades, and experienced optical workers have become used to them and accumulated considerable experience in working with them. In the case of the replacement of the machine tools, the experience acquired in working with them is lost and there arises the necessity of additional training of the optical fabricators.

The automation method based on controlling the pressure of a small tool is free of these drawbacks. Any optical machine tool used in industry can be employed without substantial reworking for the realization of this method.

Controlling the Tool Pressure

In one of the first attempts to achieve control of the material removal by means of varying the pressure [4], the control effect was not obtained. The reason was found in the fact that a full-sized tool was employed. It is obvious that in a pressure control mode, it is necessary to use a small tool, the theory for which was developed in [7, 8 and 11].

We shall pose the following problem. By means of real time control of the local pressure of a small tool on a component in a conventional optical machine tool, it is necessary to gain the capability of fabricating optical surfaces of high quality and eliminate any errors. Let the tolerance of the component have the form h(x, y). In accordance with formula (1), it is necessary to produce a force p(x, y) in the form:

$$p(x, y) = h(x, y)/KT\psi(\rho). \tag{2}$$

Here ρ is the current radius of the zone; the function $\psi(\rho)$ determines the material removal at a constant pressure [12]; K is a technological constant; and T is the machining time. In the derivation of formula (2), we neglect the finite size of the tool, but experiments conducted by us show that this method can be successfully employed.

The most important merits of the method are: the capability of automating any optical machine tool without substantially reworking it; automation simplicity using a computer in the control mode; the possibility of machining components with a complex shape and eliminating any types of errors; the absence of edge effects related to the use of a small tool.

Because of the convergence of the shaping process being controlled, the finishing operation can be accelerated by tens of times, and it is also possible to improve the quality of the finished component by several times.

Conclusion

The process of shaping optical surfaces can be automated in many ways, but it is preferable to employ real time control of the local pressure of a small tool on the component using a control computer. When this method is used, there is no need to manufacture new models of optical machine tools or complex tools.

Because of the use of the conventional motion of the tool over the surface of the part (spindle rotation and harmonic oscillation of the upper link) in the proposed control system, edge effects related to a small tool do not arise. It proves possible to fabricate components with a complex shape and eliminate any types of errors in the optical surface. The technical automation equipment existing at the present time permit the solution of this problem. Laboratory and plant tests of a bread-boarded system which realizes the principle cited here have demonstrated the promise of this approach.

BIBLIOGRAPHY

1. Beskin, G.M., et al., IZV. SPETS. ASTROFIZ. OBSERV. [PROCEEDINGS OF THE SPECIALIZED ASTROPHYSICAL OBSERVATORIES], 1975, Vol 7, p 182.

2. Vitrichenko E.A., Katagarov F.K., Lipovetskaya V.G., IZV. SPETS. ASTROFIZ. OBSERV., 1975, Vol 7, p 167.

3. Vitrichenko E.A., ASTRON. ZHURN. [JOURNAL OF ASTRONOMY], 1976, Vol 53. p 660.

4. Dvornikov A.M., et al., OMP [OPTIKO-MEKHANICHESKAYA PROMYSHLENNOST' - [THE OPTICAL MECHANICAL INDUSTRY], 1960, No 11, p 4.

5. Krupenkova Z.I., Grudina M.T., Belous R.S., OMP, 1973, No 9, p 30.

6. Leonova V.B., "Avtomatizatsiya raschetov opticheskikh sistem" ["Automating the Calculations of Optical Systems"], Moscow, Mashinostroyeniye Publishers, 1970.

7. Lysyannyy Yu.K., OMP, 1972, No 7, p 5.

8. Lysyannyy Yu.K., OMP, 1974, No 5, p 21.

9. Lysyannyy Yu.K., Tsesnek L.S., OMP, 1973, No 7, p 51.

10. Popov G.M., Popova M.B., OMP, 1970, No 3, p 46.

11. Semibratov M.N., OMP, 1958, No 9, p 37.

12. Semibratov M.N., "Spravochnik tekhnologa-priborostroitelya" ["The Instrument Builder's Handbook"], Moscow, Mashgiz, 1962, Chapter 8.

13. Tsesnek L.S., OMP, 1970, No 8, p 60.

14. Aspden R., US Patent, 1971, No 3.556.574.

15. Aspden R., French Patent, 1971, No 1.601.546.

16. Aspden R., McDonough R., Nitchie F.R., APPL. OPT., 1972, Vol 11, No 12, p 2,739.

17. Dutton D., Cornelo A., Latta M., APPL. OTP., 1968, No 7, p 125.

18. Munnerlin C.R., Teyssier C.H., OPTICAL SPECTRA, 1975, Vol 9, No 13, p 3,234.

19. Philbert M., OPTICA ACTA, 1967, Vol 14, No 2, p 169.

20. Preston F., MACHINES JOURN. OF THE SOC. OF GLASS TECHNOLOGY, 1927, Vol 20, No 2.

21. Preston F., THE GLASS INDUSTRY, 1928, Vol 9, No 2, p 3.

22. Shulte D.H., APPL. OPT., 1968, Vol 7, No 1, p 119.

23. Wilson R.G., APPL. OPT., 1975, Vol 14, No 1, p 2,286.

24. Bubis I.Ya., Kuznetsov A.I., Rozov V.Ya., OMP, 1974, No 11, p 80.

25. Zverev V.A., et al., OMP, 1977, No 2, p 18.

26. Zverev V.A., et al., OMP, 1977, No 3, p 3.

27. Zverev V.A., et al., OMP, 1977, No 4, p 3.

28. Cheban Yu.V., et al., "Novaya tekhnika v teleskopostroyenii" ["New Equipment in Telescope Construction"], 1978, No 6.

29. Jones R.A., APPL. OPT., 1947, Vol 16, p 257.

30. Marechal A., REV. D'OPT., 1977, Vol 26, p 257.

8225
CSO: 8144/976

PHYSICS

UDC 681.7.02

THE SELECTION OF THE CONDITIONS FOR THE MACHINING OF LARGE OPTICAL COMPONENTS

Leningrad OPTIKO-MEKHANICHESKAYA PROMYSHLENNOST' in Russian No 11, 1978 pp 45-49

[Article by candidate in the sciences A.P. Bogdanov, Phd. in the sciences L.S. Tsesnek, and V.A. Ivanov, manuscript received 14 March, 1978]

[Text] Questions of the choice of ways of machining optical components with large overall dimensions are analyzed. A procedure is described for selecting the machining conditions, the basis of which is an elementary law governing the wear and a gradient method of seeking the minimum of a function of several variables.

Increasing the precision and curtailing the time and labor intensity of the fabrication of the surfaces of large optical components is usually related to the precision in forecasting their wear during grinding and polishing.

Although new methods of machining large components with a "mask", a flexible tool [1] are beginning to find application in practice, a study of the possibility of controlling the process of shaping surfaces on existing machine tools by means of calculating the machining modes is of unquestionable theoretical and practical interest. It is also important to perform such research for the case of machining small optical components, including modular ones, since the kinematic characteristics of the machine tools are practically the same in both cases. We shall assume that the optical machine tool during the machining process provides for constant angular rotational velocities of the component $\overline{\Delta}$ and the tool $\overline{\omega}$, as well as oscillations of the surface of the tool either in some plane parallel to the axis of the component and offset from it by a spacing B, or around some axis which is parallel to the axis of the part. In the projection onto a plane perpendicular to the axis of the part, the indicated types of trajectories of the center of the tool are shown in Figure 1.

We shall assume that the quantity E, which in accordance with the type of trajectories indicated characterizes the displacement of the center of the tool with respect to the center of oscillations in the direction of the plane of oscillations of the tool center, or perpendicular to a straight line which passes through the point O_1 and O', changes in accordance with the sinusoidal law:

$$E = A \sin r(t + t_0)$$

where r, A, t and t_0 are respectively the angular frequency of the oscillations, the amplitude of the oscillations, the machining time, and a constant, which without violating the generality of the arguments can be considered equal to zero.

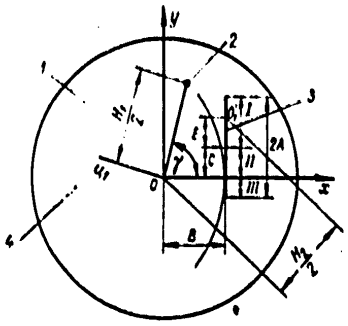

Figure 1. For the explanation of the form of the trajectories:

Key: 1. Optical part;
2. An arbitrary point on the part;
3. Trajectory 1;
4. The center of the oscillations of trajectory 2.

We shall characterize the machining mode by the set of values of the parameters Ω, ω, r, A, B, C and D. We shall conditionally understand the control of the machining process to be the selection from the specified ranges of values of the indicated parameters of the machining mode which provides for a minimum of the sum of deviations of the design value for material removal from the requisite value, expressed in terms of the absolute magnitude, at all points on the surface of the optical part.

The wear of the surface of an asperical part with small deviations from a sphere in the direction to its normal at the point $H_1/2$ for a fixed value of $H_2/2$ (Figure 1), assuming that the elementary law governing the wear in accordance with the results of paper [2] is observed, can be represented in the form:

$$h\left(\frac{H_1}{2}, \frac{H_2}{2}, V\right) = 2C_m \int_0^{\varphi} P\left(\frac{H_1}{2}, \frac{H_2}{2}, \varphi\right) l\left(\frac{H}{2}\right) \times U\left(\frac{H_1}{2}, \frac{H_2}{2}, \varphi, V\right) d\varphi, \quad (2)$$

where V is the rate of travel of the center of tool O_1, the components on the OX, OY and OZ axes are V_x, V_y and V_z (shown in Figure 1 is a picture of the points of the part and the tool in the OXY plane); P and U are the contact pressure and the relative velocity at the point $H_1/2$ and ϕ of the surface of the part respectively; C_m is a constnat for the given

machining mode; ϕ_0 is a fixed value of the angle ϕ; H/2 is half of the diameter of a circle at the surface of the tool which passes through the point $H_1/2$, ϕ of the surface of the part with the center located on the OO_1 axis; $l(H/2)$ is a coefficient which shows what part of the indicated circle belongs to the working surface of the tool.

It was assumed in deriving formula (2) that the wear within the bounds of one annular zone of the optical part is the same, i.e., it does not depend on the angle ϕ. The formula for the velocity $U(H_1/2, H_2/2, \phi, V)$, which enters into formula (2), has the following form:

(3)

where $$U = \sqrt{U_x^2 + U_y^2 + U_z^2},$$

$$\begin{aligned} U_x &= -\Omega y - (z - z_{0_1})\omega_y + (y - y_{0_1})\omega_z - V_{0_1 x}, \\ U_y &= \Omega x - (x - x_{0_1})\omega_z + (z - z_{0_1})\omega_x - V_{0_1 y}, \\ U_z &= (y - y_{0_1})\omega_x + (x - x_{0_1})\omega_y - V_{0_1 z}. \end{aligned} \tag{4}$$

The quantities x_{0_1}, y_{0_1} and z_{0_1} incorporated in formula (4), for example, for a trajectory of the first kind can be computed from the following formulas (Figure 1):

$$x_{0_1} = B, \; y_{0_1} = \pm \sqrt{\left(\frac{H_2}{2}\right)^2 - B^2},$$

where the + or - signs are taken depending on whether the center of the tool is located in the positive or negative half-plane OXY with respect to Y:

$$\begin{aligned} z_{0_1} &= R^2 - (x_{0_1}^2 + y_{0_1}^2), \; V_{0_1 x} = 0, \\ V_{0_1 y} &= Ar \operatorname{sign}(y_{0_1} - C) \cos\left[\frac{(y_{0_1} - C)}{A}\frac{\pi}{2}\right], \\ V_{0_1 z} &= -V_{0_1 y} \operatorname{tg}\left(\frac{y_{0_1}}{\sqrt{R^2 - B^2}}\right), \end{aligned} \tag{5}$$

(C can assume both positive and negative values).

The wear of the surface of the part at the point $H_1/2$ in the machining process considered here for the first kind of trajectory can be computed from the formula:

$$h\left(\frac{H_1}{2}\right) = \int_{\sqrt{B^2 + C^2}}^{\sqrt{B^2 + (A+C)^2}} \left[h\left(\frac{H_1}{2}, \frac{H_2}{2}, V\right) + h\left(\frac{H_1}{2}, \frac{H_2}{2}, -V\right)\right] dz\left(\frac{H_2}{2}\right) + \int_{B}^{\sqrt{R^2 + C^2}} \left[h\left(\frac{H_1}{2}, \frac{H_2}{2}, V\right) + \right.$$

$$+h\left(\frac{H_1}{2}, \frac{H_2}{2}, V\right)\Big]d\tau\left(\frac{H_2}{2}\right)+$$
$$+\int_{B}^{\sqrt{B^2+(A+C)^2}}\left[h\left(\frac{H_1}{2}, \frac{H_2}{2}, V\right)+\right.$$
$$\left.+h\left(\frac{H_1}{2}, \frac{H_2}{2}, -V\right)\right]d\tau\left(\frac{H_2}{2}\right), \quad (6)$$

where the I, II and III being compared correspond to the I, II and III sections of the trajectory (Figure 1); $d\tau(H_2/2)$ is the time the center of the tool O_1 is located at the point $H_2/2$. The arguments are similar for the second kind of trajectories.

The time $d\tau(H_2/2)$ can be expressed in terms of the parameters indicated above by means of the formula:

$$d\tau\left(\frac{H_2}{2}\right)=\frac{dy_{O_1}}{V_{O_1 y}},$$

In which the numerator and denominator correspond to the position of the center of the tool characterized by the coordinates (5).

Thus, with the assumptions made here in the symbols adopted, the set of values of the parameters Ω, r, ω, A, B, C and D correspond to an efficient machining mode when they satisfy the equality:

$$\int_0^{D_1/2}\left|h\left(\frac{H_1}{2}\right)-h^3\left(\frac{H_1}{2}\right)\right|d\left(\frac{H_1}{2}\right)=$$
$$=\Phi_1(\Omega, r, \omega, A, B, C, D)=\min, \quad (7)$$

where $h^3(H_1/2)$ is the requisite material removal from the surface of the optical part.

We shall search for this minimum in the following fashion, taking into account the fact that in the range of variation in the parameters Ω, r, ω, A, B, C and D, generally speaking, there can exist a number of local minima of expression (7). The range of variation of each of the parameters is broken down into subranges, which are equal for the sake of definiteness. Taking the centers of the subranges as the values of the parameters, we compile all possible sets of these values, excluding only those which do not satisfy the machining process, for which:

$$\sqrt{(A+C)^2+B^2}\geqslant\frac{D_1}{2}-\rho_1,$$

where ρ_1 is the minimum permissible spacing between the center of the tool and the edge of the part.

Further, taking the sets indicated here sequantially as the initial approximations, the minima of the function $\Phi_1((\Omega, \omega, r, A, B, C, D)$ are

sought by the gradient method of [3]. The set corresponding to the least of them

$$\omega = \omega_p,\ \Omega = \Omega_p,\ r = r_p,$$
$$A = A_p,\ B = B_p,\ C = C_p,\ D = D_p$$

is taken as the desired solution. The volume of calculation work in searching for the minimum of function (7) can be curtailed if the following function is formula (6):

$$h\left(\frac{H_1}{2}, \frac{H_2}{2}, V(V_x, V_y, V_z)\right)$$

is represented in a Taylor's series in the vicinity of the point ($H_1/2$, $H_2/2$, $V(V_x,0,0)$) or:

$$\left(\frac{H_1}{2}, \frac{H_2}{2}, V(0, V_y, 0)\right)$$

depending on whether $|V_x| \geq |V_y|$ or not:

$$\begin{aligned}
&h\left(\frac{H_1}{2}, \frac{H_2}{2}, V(V_x, V_y, V_z)\right) = \\
&= h\left(\frac{H_1}{2}, \frac{H_2}{2}, V(V_x, 0, 0)\right) + \\
&\quad + b_1(V_x) V_y + C_1(V_x) V_z, \\
&h\left(\frac{H_1}{2}, \frac{H_2}{2}, V(V_x, V_y, V_z)\right) = \\
&= h\left(\frac{H_1}{2}, \frac{H_2}{2}, V(0, V_y, 0)\right) + \\
&\quad + a_1(V_y) V_x + C_2(V_y) V_z,
\end{aligned} \tag{8}$$

where $C_1(V_x)$, $b_1(V_x)$, $a_1(V_y)$, and $C_2(V_y)$ are certain constant coefficients.

To calculate the values of the function $h(H_1/2, H_2/2, V(V_x,V_y,V_z))$, it is necessary to compute the values $h(H_1/2, H_2/2, V(V_x,0,0))$ and $h(H_1/2, H_2/2, V(0,V_y,0))$ beforehand for fixed values of V_x and V_y from the region of their variation, as well as the coordinates $a_1(V_y)$, $b_1(V_x)$, $C_1(V_x)$ and $C_2(V_y)$, and to list them in a table.

The values of the functions (8) should be computed by using the property of their monotonicity in the following manner. We shall determine the first term on the right sides of equations (8) from the data of the indicated table, assuming that the values:

$$h\left(\frac{H_1}{2}, \frac{H_2}{2}, V(V_x, 0, 0)\right),$$
$$h\left(\frac{H_1}{2}, \frac{H_2}{2}, V(0, V_y, 0)\right)$$

in the intervals between two adjacent tabular values change in accordance with a linear law. The remaining terms are found by means of the table coefficients.

Table: Grinding Modes for a Mirror with a Diameter of 1,260 mm

A, mm	B, mm	C, mm	
300	50	0	28
300	70	0	27
290	80	0	32
250	410	0	1
220	80	0	28
50	223	0	10
110	223	0	8
400	200	0	18
110	223	0	8
190	98	0	8
110	260	0	10
110	230	0	8
110	223	0	8
110	230	0	8
110	240	0	6
110	223	0	7
150	223	0	7

The proposed procedure for the calculations of the machining modes for large optical components was run on a "Minsk-32" electronic digital computer. A spherical mirror with a diameter of 1,260 mm and a radius of the sphere equal to 50,000 mm was ground, and a large parabolic reflector was polished. The first of the reflectors indicated was machined with a tool having a diameter of 850 mm. In both machining instances, the center of the tool moved along a trajectory of the first kind. The range of variation in the values of the parameters Ω, A, B and C in the first machining case were as follows:

$$0.15 \leq \Omega \leq 5 \text{ r.p.m.}; \quad 0 \leq r \leq 9 \text{ dv.kh/min [unknown units per minute]};$$

$$0 \leq A, B, C \leq 630 \text{ mm}.$$

The precision which was achieved is characterized by a maximum deviation of the actual shape of the surface from that required amounting $\pm$ 0.6 μm. After this, the grinding was terminated. Shown in Figures 2 and 3 are curves K1--K18 (K1 is the original curve) which characterize the deviations of the actual shape of the surface from that required over 17 machining sessions, and the machining modes are given in the table. The radius of the requisite surface shape following each machining session was imprecisely determined, since the requirements placed on the precision of its determination were not high. Calculations showed that the curves $h(H_1/2)$ are smooth, with no more than two maxima, and by selecting the machining mode using the procedure proposed here, and executing a number of grinding sessions, one can assure a reliable approximation of the actual shape of the surface to that required.

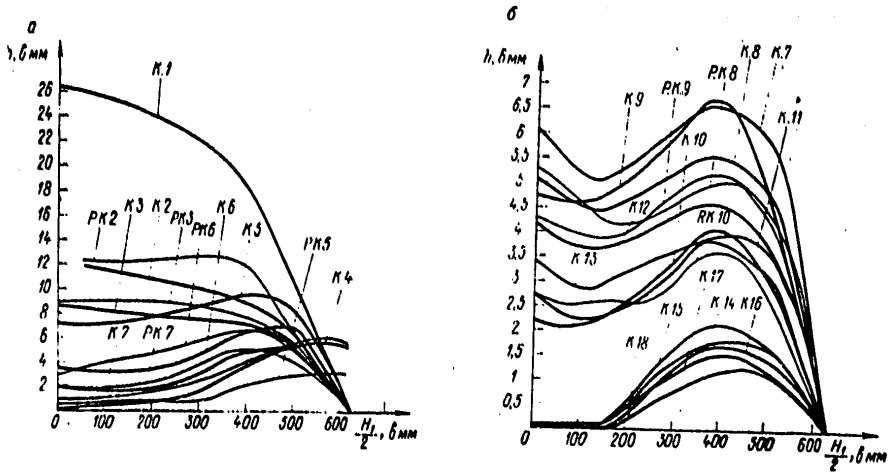

Figure 2. Curves characterizing the deviation of the actual shape of the mirror surface from that required.

Along with this, a redistribution of the contact pressure occurs during the grinding process in the region of contact between the surface of the part and the tool, due to the excursion of the tool beyond the edge of the part. Thus, in the fourth and eighth sessions (the i-th session effects the transition from one surface shape to another, which is characterized by the i-th and the (i + 1)-th curves), which were also designated for the purpose of determining the permissible excursion of the tool beyond the edge of the part and the departure in which was equal to more than 212 mm, it was recorded that the design value of the wear differed from the actual wear (the actual was greater than the design value) at the points $H_1/2$ = = 450 mm and 625 mm by 1.35 and more than 2.7 times respectively. In the eleventh session, during an excursion of the tool of 82 mm, differences at the points cited above were recorded in the amount of 1.25 times and 1.9 times greater, while in the majority of the remaining sessions, when $r/\Omega \leq 10$ and the excursion amounted to about 50 mm, the differences were 1.2 and 1.5 times greater respectively. The differences in the predicted surface shape, which are characterized by the P, K and i curves can be seen in Figures 2 and 3.

Since the laws governing the surface wear of the part when the tool runs out beyond its edge are stable ones, two cases of accounting for this are of interest: replacing $h(H_1/2)$ in formula (7) by $h(H_1/2)k(H_1/2)$, where $k(H_1/2)$ are coefficients which have to be determined experimentally, as in the grinding variant considered here (such accounting, as shown in Figure 3, permits successfully dealing with a difficulty traditional for optical workers - the elimination of the "hump" in front of the edge of

the part); the determination of the design value for the wear $h(H_1/2, H_2/2, V)$ and $h(H_1/2, H_2/2, -V)$ taking into account the nonuniformity in the distribution of the contact pressures, based on methods for solving contact problems in the shaping of optical surfaces. During the polishing of the part in different machining sessions, the instability in the rotational speed of the tool was registered in a wide range (the size of the velocity varied by three times, while the direction changed to the opposite direction). With large swings in the oscillations of the tool (2A), such instability leads to errors in the predicting of the surface shape.

To increase the precision in forecasting the shape of the surface during polishing, it is expedient to stabilize the angular rotational of the tool.

BIBLIOGRAPHY

1. Tsesnek L.S., OMP [THE OPTICAL MECHANICAL INDUSTRY], 1970, No 8, p 60.

2. Bogdanov A.P., Tsesnek L.S., OMP, 1976, No 3, p 42.

3. Korn G., Korn T., "Spravochnik po matematike dlya nauchnykh rabotnikov" ["Mathematics Handbook for Scientific Workers"], Moscow, Nauka Publishers, 1973.

8225
CSO: 8144/976

PHYSICS

UDC 669.018.28; 669.018.472

CAST COMPONENTS OF SUPERINVAR FOR OPTICAL INSTRUMENTS*

Leningrad OPTIKO-MEKHANICHESKAYA PROMYSHLENNOST' in Russian No 11, 1978 pp 49-51

[Article by S.V. Rabinovich, Candidate of the Sciences R.A. Sidorenko, M.D. Kharchuk, and Candidate of the Sciences A.Ya. Ioffe, manuscript received 3 April, 1978]

[Text] The use of structural materials which have a minimum temperature coefficient of linear expansion (TKLR) is essential in assuring operational precision in a climatic range of temperatures of devices for various purposes. The correct choice of metal materials with a specified TKLR is of particular importance for the fabrication of mountings for optical components.

When using materials with a TKLR close to that of glass, the minimum level of stresses is maintained in the glass, to which the abscence of distortions in an optical system is related. To fabricate metal components which operate in conjunction with quartz glass, the use of superinvar (alloy 32NKD, GOST [State Standard] 10994-64) is the most promising. Its TKLR does not exceed $1 \cdot 10^{-6}$ deg^{-1}, which is very close to the TKLR of quartz glass ($0.2--0.5\ 1 \cdot 10^{-6}$ deg^{-1}, GOST 15130-69), but the 32 NKD alloy is supplied only in the form of roll stock, something which because of the poor machinability limits the possibility of using this alloy, especially for parts with a complex shape. In this regard, the production of cast parts from 32 NKD alloy is an extremely urgent problem for the mechanical optics industry, since it allows for expanding the products list and sharply reducing the labor intensity of component fabrication.

The necessity arose in the mastery of shaped casting from the 32 NKD alloy to carry out a number of studies, since its special features were ascertained, such as the presence of a cellular substructure and a considerable tendency

---

* E.Ya. Kaufman and L.M. Lunina participated in the work.

to form hot cracks. The liquation of the major components of the alloy with respect to the cross-section of the cells was studied with the "Kameka-MS-46" X-ray spectrum analyzer. It was determined that nickel and copper liquate at the boundaries, while cobalt does so towards the center of the cells at a maximum scatter in the concentrations of 4, 0.4 and 0.5% respectively (for samples with a diameter of 10 mm). Because of liquation of the elements over the cross-section, a cellular substructure is undesirable, and for this reason, conditions were found under which it is not formed. Samples of 32 NKD alloy were melted by the method of zonal melting with hardening rates of from 0.55 to 8 mm/min. The trials were carried out using an "Kristall DM" installation in a vacuum ($5 \cdot 10^{-5}$ torr). It was found that the cellular substructure for samples of with a diameter of 5-7 mm does not arise at hardening rates which do not exceed 1 mm/min.

TABLE 1

The Chemical Composition of the Casting Alloy 32 NKD

Element	Element Content by Weight, %	Element	Element Content by Weight, %
Nickel	33-32.5	Rare earth from the group: cerium, lanthanum, praseodymium, neodymium, total	0.04--0.20
Cobalt	3.2--4.2	Sulfur	$\leq$ 0.02
Copper	0.6--0.8	Phosphorous	$\leq$ 0.02
Silicon	0.02--0.15	Iron	Remainder

It is well known that to eliminate a cellular substructure, it is necessary, along with a minimum hardening rate, to have a maximum temperature gradient [1], but for the cast alloy NKD, such conditions are hardly feasible in practice when using the methods of shaped casting used in industry. In this regard, further research was carried out to determine the chemical composition of the cast alloy which assures the working characteristics where the cellular substructure is present.

The chemical composition of the alloy was determined for the fabrication of shape castings using investment patterns (Table 1) [2], which provide for a TKLR of no more than $1 \cdot 10^{-6}$ deg^{-1} in a temperature range of $\pm$ 100° C

TABLE 2

The Statistical Processing of the Results of Measuring the Temperature Coefficients of Linear Expansion of Cast Superinvar as a Function of the Nickel Content

(1) Содержание никеля, вес. %	(2) ТКЛР, град$^{-1}$ · 10^{-6} в интервале 20—100 °С	(3) Число замеров	(4) Доверительный интервал, град$^{-1}$ · 10^{-6}	(5) Доверительная вероятность
31,15	1,01	9	±0,3	0,71
31,75	0,73	11	±0,27	0,57
32,0	0,53	20	±0,47	0,77
32,3	0,43	10	±0,57	0,97
32,6	0,38	31	±0,62	0,983
32,9	0,45	21	±0,55	0,999
33,2	0,47	35	±0,53	0,94
33,5	0,68	11	±0,32	0,73
33,8	0,75	14	±0,25	0,68
34,0	0,99	10	±0,3	0,89
35,0	1,35	9	±0,3	0,53

Key: 1. Nickel content by weight, %;
2. Temperature coefficient of linear expansion, deg^{-1} · 10^{-6} in a range of 20--100° C;
3. Number of measurements;
4. Confidence interval, deg^{-1} · 10^{-6};
5. Confidence level.

Notes: 1. For alloys with a TKLR of less than 1 · 10^{-6} deg^{-1}, the confidence interval was chosen so as to determine the confidence level fro obtaining a TKLR of no more than 1 · 10^{-6} deg^{-1}.

2. Samples having deviations in the nickel content of ± 0.15% were combined in one group as regards nickel content;

3. The content of the remaining components (by weight, %): Co 3.37--4.0; Cu 0.48--0.93; C 0.01--0.028; Si 0.037--0.15; S ≤ 0.02; P ≤ 0.02.

4. The statistical processing was performed in accordance with the procedure described in the literature [3].

as well as optimum production technology properties. It was determined that the minimum TKLR of the alloy is achieved when the nickel content is increased by 0.5% (Table 2) as compared to the rolled product (GOST 10994-64). The introduction of rare earth metals permitted an increase in the cracking resistance of the alloy. An investigation of the influence of cerium, lanthanum, yttrium and the MTs75 and MTs40 mixed metals showed that the maximum crack resistance was assured when rare earth metals were introduced in

the form of mixed metal MTs40 in the amount of 0.25% of the weight of the charge. The mechanical properties of the alloy were studied using samples fabricated by investment pattern casting, and their average values are given in Table 3.

TABLE 3

The Mechanical Properties of 32NKD Casting Alloy

(1) Температура испытания, °C	(2) Временное сопротивление разрыву, кгс/мм²	(3) Предел текучести, кгс/мм²	(4) Относительное удлинение, %	(5) Относительное сужение, %	(6) Ударная вязкость, кгс·м/см²
−100	59,0	41,0	20,0	30,0	8,0
−60	52,5	30,5	23,5	42,6	8,0
20	40,5	25,0	23,0	50,0	12,5
100	33,0	20,0	22,5	46,5	16,0

Key: 1. Test temperature, °C;
2. Tensile strength, kgf/mm^2;
3. Yield point, kgf/mm^2;
4. Percentage elongation, %;
5. Relative reduction, %;
6. Impact strength, kgf · m/cm^2;

Notes: 1. Samples in accordance with GOST 1497-61, 1150-65 and 9456-60. The tensile tests were performed on an IM-4R machine at a rate of 1.25 mm/min. Five samples were tested at each temperature. To determine the impact strength, seven samples each were tested on an MK-30 pendulum hammer in accordance with GOST 9455-60 and 9456-60;

2. The chemical composition of the alloy from which the samples were fabricated (by weight, %): Ni - 32.9; So - 3.7; Si - 0.12; Cu - 0.73; Mn - 0.32; Ce - 0.061; La - 0.031; S - 0.02; P - 0.02; C - 0.027; F - the remainder.

The industrial process for melting 32NKD alloy for shaped casting manufacture does not differ as a whole from the production technology adopted for precision nickel-iron alloys, and there are only a few special features. The melting in the open high frequency induction furnace should be forced. For complex castings, it is desirable to perform the melting and pouring in a vacuum. The MTs40 mixed metal is introduced into a ladel under a jet following the preliminary deoxidation of the alloy, for which ferromanganese, ferrosilicon and aluminum were used in our case. The temperature for filling the patterns was 1,510--1,550°. Using the developed technology,

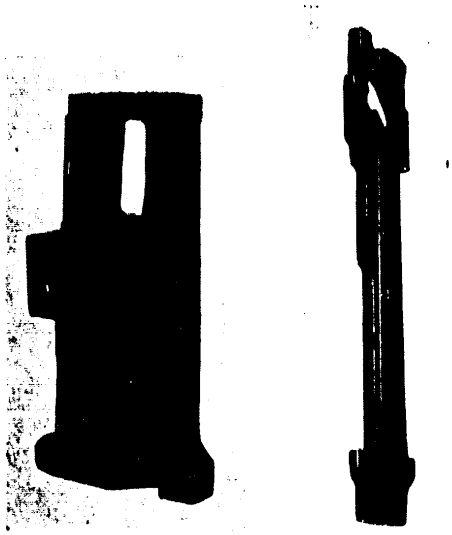

Castings of the 32NKD alloy.

Shaped castings for five designations were fabricated, two of which are shown in the figure; the mass of the castings was 0.25--1.7 kg, and the thickness of the walls was 4--15 mm.

BIBLIOGRAPHY

1. Chalmers B., "Teoriya zatverdevaniya" ["The Theory of Freezing"], Moscow, Metallurgiya Publishers, 1968, p 153-162.

2. Ioffe A.Ya., et al., Patent No. 501111, BYUL. IZOBR. [BULLETING OF INVENTIONS], 1976, No 4.

3. Zaydel' A.N., "Oshibki izmereniy fizicheskikh velichin" ["Errors in the Measurement of Physical Quantities"], Leningrad, Nauka Publishers, 1974.

8225
CSO: 8144/976

PHYSICS

UDC 551.521.3:593.52

THE STATISTICAL CHARACTERISTICS OF OPTICAL RADIATION ATTENUATION IN THE GROUND LAYER OF THE ATMOSPHERE (SPRING, AUTUMN)

Leningrad OPTIKO-MEKHANICHESKAYA PROMYSHLENNOST' in Russian No 11, 1978 pp 58-62

[Article by V.L. Filippov, V.P. Ivanov and A.S. Makarov, manuscript received 16 November, 1977]

[Text] The main statistical characteristics of data obtained in the study of aerosol attenuation of visible and infrared radiation in hazes, foggy hazes and hazes with drizzle are analyzed.

Despite the increased volume of information in recent years concerning the variability of the spectral optical density of aerosols under various weather conditions, the feasibility and confidence level of the forecasting of the IR transmittance of a turbid atmosphere from the data of measurements in the visible range of the spectrum, remain, as before, disputed issues. The problem takes on particular urgency when discussing the permissibility of extrapolating the data of local measurements to regions with similar geographical and climatic conditions. Taking this into account, the authors consider it expedient to continue the discussion of the materials obtained, beginning in 1970.

Considering the conclusions of a number of authors of the considerable weakening of the correlation between variations ofthe coefficients α_λ in the visible range of the spectrum and when $\lambda \geq 2$ μm, the range of wavelengths which is discussed in this paper, without damaging the qualitative information contained in the material as a whole, was limited to $\lambda = 0.55—6.0$ μm, and the aerosol attenuation factors were determined in the transmittance "windows" close to wavelengths of 0.55, 0.83, 1.06, 1.18, 1.66, 2.09 and 3.97 μm. The weather conditions considered here are associated with the spring and autumn periods. A comparatively large diversity of optical conditions is characteristic of the ground layer of air, where these conditions cannot be successfully described by a single model, even in the case where the modeling encompasses only individual characteristics of the medium, as for example, the spectral dependence and variability of the radiation attenuation factors in a broad range of the spectrum.

The analysis of the results of the experimental studies of the variations of the aerosol attenuation factors shows that for the spring and autumn periods, the majority of recorded spectral relationships $\alpha = \phi(\lambda)$ can be associated with four qualitatively different classes, types of "optical weather" [2]: haze, foggy haze, fog and haze with drizzle. We shall consider in particular the analysis of the results of the statistical processing of the spectral functions of the aerosol attenuation factors for hazes, hazes with drizzle and foggy hazes. Based on the conditions of the experiment, the factors are:

$$\alpha_\lambda = -\frac{\ln \tau_\lambda}{L},$$

where τ_λ is the spectral transmittance in the range of λ; L is the length of the optical path, specified by a finite number of spectral points. This means that the result of a single measurement of the attenuation factors, which takes the form of a random function [3], can be treated as the realization of an n-dimensional vector, where n is the number of values of λ chosen over the spectrum. The main statistical characteristics of this vector will be the average values:

$$\bar{\alpha}_{\lambda_i} = \frac{1}{N}\sum_{l=1}^{N} \alpha_{l\lambda_i}$$

(N is the number of realizations in the sample statistical ensemble), the correlation matrix is:

$$B[\Delta\alpha_{\lambda_i}\Delta\alpha_{\lambda_k}] = \frac{1}{N}\sum_{l=1}^{N}\left(\alpha_{l\lambda_i} - \bar{\alpha}_{\lambda_i}\right)\left(\alpha_{l\lambda_k} - \bar{\alpha}_{\lambda_k}\right)$$

or the normalized correlation matrix is:

$$\rho_{\lambda_i\lambda_k} = \frac{B[\Delta\alpha_{\lambda_i}\Delta\alpha_{\lambda_k}]}{\sigma_{\lambda_i}\sigma_{\lambda_k}} \quad (l = 1, 2, \ldots, N;\ i, k = 1, 2, \ldots, n),$$

where the dispersion is

$$\sigma^2_{\lambda_i} = B_{\lambda_i\lambda_i}.$$

The average spectral functions $\bar{\alpha}_\lambda$, which determine the conditions for hazes ($N = 700$, 3 km $\leq S_M \leq$ 20 km, 40% $\leq f \leq$ 90%), hazes with drizzle ($N = 150$), and foggy hazes ($N = 300$, 1 km $\leq S_M \leq$ 10 km, $f >$ 90%) in various weather situations, which can be characterized by specified limits on the meteorological visibility range S_M and the relative humidity f, are shown in the figure. The results of calculating the normalized correlation matrices for the statistical ensembles indicated above are illustrated in Table 1 (A is for hazes, B for fogs, and C for hazes with drizzle). Table 2 contains the corresponding estimates of the confidence intervals, computed for empirical correlation coefficients of $\rho_{0.55;\ \lambda(k)}$.

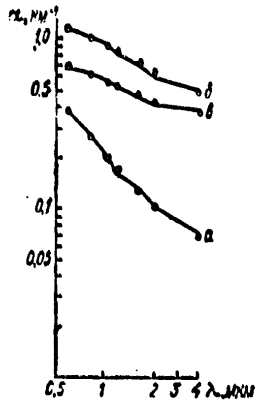

Figure: The spectral curves of the aerosol attenuation factors $\overline{\alpha}_\lambda$ under the following conditions:
a. Haze;
b. Foggy haze;
c. Haze with drizzle;
The small circles are the calculation results.

The data of Tables 1 and 2 indicate that for the aerosol states of the atmosphere studied here, a characteristic feature is the close interrelationship between the variations $\Delta\alpha_\lambda$ in various sections of the spectrum, including where $\lambda = 0.55 -- 2$ μm and $\lambda > 2$ μm. The information obtained with this contradicts the conclusions of the authors of papers [1, 4, 5], in accordance with which the observed substantial weakening of the correlation between variations in the "aerosol transmittance" of the atmosphere in the visible and IR regions of the spectrum is related to the difference between the sources and mechanisms for the transformations of finely dispersed particle fractions which are responsible for the attenuation of radiation in the visible range and the large dispersed aerosols which determine the attenuation of IR radiation (in our case, the somewhat lower values of the correlation coefficients $\rho_{\lambda_i\lambda_k}$ in the Table (A) are undoubtedly primarily due to the measurement errors of the optical density of the hazes, the average value of which for $\lambda > 1$ μm was ≤ 0.1).

Thus, the measurement results permit once again noting the fact that the problem of reproducing the spectral curve of the aerosol attenuation factors α_λ on the basis of measurements of $\alpha_{0.55}$ or S_M has a good basis.

The results of a quantitative comparison of the characteristics obtained touch on a second important aspect, where these characteristics correspond to the conditions of the Zvenigorodsk scientific station of the Institute of Atmospheric Physics of the USSR Academy of Sciences [1, 2]. This circumstance gives direct evidence of the fact that the processes of the conversion of aerosol formations in the regions of the measurements are likewise the same. Also to be taken into account is the fact that the justification for the conclusions reached follows from the results of the synchronous measurements of variations in the dispersion composition of the aerosols for the case of particle sizes from 0.1 to 10 μm [6]. The latter have shown that in the process of forming a foggy haze, the large dispersed fraction of the aerosols is primarily formed as a result of the condensation-coagulation growth of the smallest particles ($r \leq 0.1 -- 0.8$ μm).

With the "breaking up" of a foggy haze, the large aerosols upon evaporating again change over to the region of small particles, i.e., the attenuation of radiation in both the visible and IR regions of the spectrum is apparently due to particles of an identical nature.

TABLE 1

	λ_i, мкм	λ_k, мкм 0,55	0,83	1,06	1,18	1,66	2,09	3,97	$\bar{a}_\lambda$, км$^{-1}$	σ_1^2
	0,55	1,0	0,954	0,913	0,896	0,874	0,838	0,800	0,380	0,031
	0,83		1,0	0,952	0,938	0,911	0,869	0,833	0,275	0,025
	1,06			1,0	0,968	0,943	0,898	0,862	0,206	0,019
А	1,18				1,0	0,978	0,940	0,901	0,165	0,016
	1,66					1,0	0,972	0,932	0,134	0,013
	2,09						1,0	0,960	0,105	0,01
	3,97							1,0	0,074	0,009
	0,55	1,0	0,998	0,996	0,994	0,988	0,979	0,950	1,115	1,853
	0,83		1,0	0,999	0,997	0,982	0,982	0,954	1,025	1,782
	1,06			1,0	0,998	0,994	0,983	0,957	0,929	1,668
Б	1,18				1,0	0,996	0,987	0,961	0,819	1,435
	1,66					1,0	0,991	0,972	0,697	1,068
	2,09						1,0	0,991	0,599	0,822
	3,97							1,0	0,508	0,699
	0,55	1,0	0,995	0,991	0,986	0,984	0,977	0,977	0,680	0,411
	0,83		1,0	0,997	0,992	0,985	0,975	0,973	0,635	0,380
	1,06			1,0	0,997	0,990	0,979	0,975	0,575	0,339
В	1,18				1,0	0,995	0,986	0,992	0,528	0,296
	1,66					0,1	0,996	0,982	0,462	0,238
	2,09						0,1	0,995	0,421	0,213
	3,97							1,0	0,391	0,136

For the purpose of obtaining more complete information on the statistical characteristics of aerosol attenuation, the eigen-values a_k and the eigen-vectors $S_k(\lambda)$ were computed for each of the correlation matrices $B[\Delta\alpha_{\lambda_i}\Delta\alpha_{\lambda_k}]$. The eigen-values a_k and the first two eigen-vectors $S_1(\lambda)$ and $S_2(\lambda)$ are given in Tables 3 and 4 respectively. It can be shown [7, 8] that even the first two eigen-vectors are sufficient to reproduce the spectral curve α_λ with an error of no more than 3%.

TABLE 2

(1) Тип ситуации	λ, мкм 0,83	1,06	1,18	1,66	2,09	3,97
(2) Дымка	± 0,01	± 0,019	± 0,022	± 0,027	± 0,033	± 0,041
(3) Туманная дымка	± 0,001	± 0,001	± 0,002	± 0,004	± 0,007	± 0,017
(4) Дымка с моросью	± 0,002	± 0,003	± 0,007	± 0,008	± 0,011	± 0,012

Key: 1. Type of situation;
2. Haze;
3. Foggy haze;
4. Haze with drizzle.

TABLE 3

K	(1) Дымка		(2) Туманная дымка		(3) Дымка с моросью	
	a_k	γ_k	a_k	γ_k	a_k	γ_k
1	0,114	93	9,23	99	2,04	99
2	0,005	97	0,075	99,6	0,014	99,5
3	0,002	98	0,012	100	0,005	100
4	0,001	99	0,005	100	0,001	100
5	0,001	100	0,002	100	0,001	100
S_a	0,123		9,326		2,061	
S_1	0,009		0,096		0,021	

Key: 1. Haze;
2. Foggy haze;
3. Haze with drizzle.

Regardless of the possibilities represented by the data of Tables 1 — 4, in practice it is frequently more convenient in calculating the coefficients of aerosol attenuation to employ the procedure proposed in [12]. For this reason, in this paper, just as in [12], the following relationship was adopted for the approximation of the mean statistical curves being discussed, which determine the spectral curve of the coefficient α_λ in the windows of atmospheric transparency:

$$\alpha_\lambda = \alpha_{0.55}[n_0 + n_1\lambda^{-n2}$$

The values of the empirical coefficients n_0, n_1 and n_2 which were obtained by the method of least squares, and which define the spectral curve of α_λ, are shown in Table 5 for $\alpha_{0.55} = 1$. The circles in the figure for the indicated weather conditions correspond to the results of calculations using the expression given here for the spectral curve of the coefficient α_λ, which attests to the good agreement of the data (the approximation error is $\leq$ 5%).

TABLE 4

λ, мкм	(1) Дымка		(2) Туманная дымка		(3) Дымка с моросью	
	$S_1(\lambda)$	$S_2(\lambda)$	$S_1(\lambda)$	$S_2(\lambda)$	$S_1(\lambda)$	$S_2(\lambda)$
0,53	0,498	—612	0,446	—0,332	0,446	—0,361
0,83	0,456	—0,296	0,439	—0,270	0,430	—0,416
1,06	0,401	0,04	0,424	—0,192	0,407	—0,247
1,18	0,367	0,231	0,394	—0,075	0,380	0,031
1,66	0,325	0,343	0,339	0,144	0,340	0,325
2,09	0,282	0,415	0,296	0,435	0,320	0,517
3,97	0,251	0,439	0,267	0,715	0,300	0,512

Key: 1. Haze;
2. Foggy haze;
3. Haze with drizzle.

TABLE 5

(1) Погодные условия (весна — осень)	n_0	n_1	n_2	Литературные данные о n_2 [15—19] (2)
(3) Дымка	0,1	0,45	1,3	1 — 1,5
(4) Туманная дымка	0,01	0,8	0,5	0,3 — 0,9
(5) Дымка с моросью	0,3	0,5	0,6	0,79

Key: 1. Weather conditions (spring-autumn);
2. Data from the literature on n_2 [15 - 19];
3. Haze;
4. Foggy haze;
5. Haze with drizzle.

The corresponding values of the more precise coefficients n_0 and n_1, and the exponent n_2 for the types of optical weather considered here are close in terms of their size to those known from the literature (see [9—13]), and also correspond to the recommendations of [12]. It is necessary to note only the difference of the quantity n_2 from Table 5, where this difference is of practical significance and related to the more careful breakdown of the initial data in this paper for the purpose of eliminating from consideration those spectra which were actually obtained under conditions of rain.

In generalizing the analysis materials presented here for the results of an orthogonal breakdown of the field of aerosol attenuation of radiation in the ground layer of the atmosphere, we shall again underscore the rightfulness of using the expression given above for the purpose of calculating the coefficients α_λ for each of the optical situations under discussion.

In conclusion, the authors consider it their duty to express their gratitude to T.V. Spiridonova for assisting in processing the measurement results on computer.

BIBLIOGRAPHY

1. Georgiyevskiy Yu.S., et al., IZV AN SSSR, FAO [PROCEEDINGS OF THE USSR ACADEMY OF SCIENCES, ATMOSPHERIC AND OCEANIC PHYSICS], 1973, Vol 9, No 6, p 655.

2. Rozenberg G.V., IZV. AN SSSR, FAO, 1967, Vol 3, No 9, p 936.

3. Pugachev V.S., "Teoriya sluchaynykh funktsiy" ["The Theory of Random Functions"], Fizmatgiz Publishers, 1962.

4. Georgiyevskiy Yu.S., IZV. AN SSSR, FAO, 1969, Vol 5, No 4, p 376.

5. Laktionov A.G., et al., IZV. AN SSSR, FAO, 1973, Vol 9, No 2, p 138.

6. Filippov V.L., et al., OMP [THE OPTICAL-MECHANICAL INDUSTRY], 1974, No 1, p 34.

7. Obukhov A.N., IZV. AN SSSR, Ser. "Geofizika" [PROCEEDINGS OF THE USSR ACADEMY OF SCIENCES, GEOPHYSICS SERIES], 1960, No 3, p 432.

8. Malkevich M.S., "Opticheskiye issledovaniya atmosfery so sputnikov" ["Optical Investigations of the Atmosphere from Satellites"], Moscow, Nauka Publishers, 1973.

9. Volz F., "Optik des Dunstes. Handbuch der Geoph." ["The Optics of Haze. Geophysics Handbook"], Edited by E. Linke and Moeller, Vol III, Borntraeger Publishers, Berlin, 1956.

10. Yunge Kh., "Khimicheskiy sostav i radioaktivnost' atmosfery" ["The Chemical Composition of the Atmosphere"], Mir Publishers, 1965.

11. Zuyev V.Ye., "Rasprostraneniye vidimykh i IK-voln v atmosfere" ["The Propagation of Visible and Infrared Waves in the Atmosphere"], Sovetskoye Radio Publishers, 1970.

12. Filippov V.L., Mirumyants S.O., IZV. VUZOV, FIZIKA [PROCEEDINGS OF THE HIGHER EDUCATIONAL INSTITUTES, PHYSICS], 1972, No 10, p 103.

13. Toropova T.P., et al., in the collection, "Pole rasseyannogo izlucheniya v zemnoy atmosfere" ["The Field of Scattered Radiation in the Earth's Atmosphere"], Alma-Ata, Publishing House of the Kazakh SSR, 1974.

8225
CSO: 8144/976

PHYSICS

UDC 621.384.326.23

A HEAT SCANNING VIEWER FOR QUALITY CONTROL IN THE ASSEMBLY OF THE STATORS OF ELECTRICAL MACHINES

Leningrad OPTIKO-MEKHANICHESKAYA PROMYSHLENNOST' in Russian No 11, 1978 pp 74-75

[Article by Phd. in the sciences M.M. Miroshnikov, R.N. Ivanva, P.P Rudakas, R.A. Zhukov, K.S. Karapetyan and T.D. Mozina, manuscript received 19 April, 1978]

[Text] In recent years, considerable attention has been devoted in our country to the introduction of nondestructive quality control methods for industrial products for testing them during fabrication and operation.

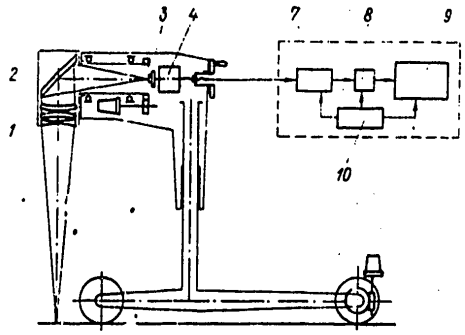

Figure 1. Functional diagram of the thermal scanning viewer

A specialized model of a thermal viewer was designed to realize the thermal viewing method of nondestructive quality control of the assembly of the stators of electrical machines, in particular, the stators of high power turbogenerators and synchronous compensators, for the purpose of ascertaining short-circuited laminations in the solid mass of steel.

A functional schematic of the heat viewer is shown in Figure 1. The rotating scanner, which incorporates the objective 1 and inclined reflector 2,

effects the element by element circular inspection of the internal surface of the stator being studied. Infrared radiation from a surface element is focused by the objective on the sensitive area of photoresistor 3. Where a temperature difference exists between two adjacent surface elements, an electrical signal is generated at the terminals of the photoresistor, which is proportional to this difference, and which following amplification in voltage amplifiers 4 and 7 and current amplifier 8, is fed to the electrodes of the recording block 9, where a line by line black and white half-tone image of the object is reproduced on electrochemical paper in the form of a "heat map."

Figure 2. A "heat map" of the interior surface of a turbogenerator stator.

Simultaneously with the amplification of the signal by gamma corrector 8, the volt-ampere characteristic of the recording block is equalized, something which permits increasing the number of visible half-tones in the image being reproduced.

With the simultaneous rotation of thescanner and the travel of the optical head at a fixed rate along the stator by means of the self-propelled chasis, the entire internal surface is sequentially examined along the threaded drive line without omissions and superimpositions.

A "heat map" of the internal surface of a turbogenerator stator is shown in Figure 2.

An uncooled photoresistor of lead selenide (SF4-1) with a sensitive area size of 1 x 1 mm is used as the radiation detector.

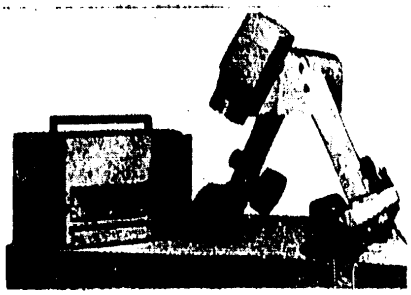

Figure 3. General view of the instrument.

The objective has three lenses (one lens is made of lithium fluoride and two are made of calcium fluoride) with a relative aperture of 1.33, a focal distance of 133.6 mm and a magnification of 0.2. The diameter of the circle of confusion in a spectral range of 1.8--4.8 μm is no more than 0.5 mm.

The heat viewer has the following technical and operational characteristics:

Angular resolution	20 angular minutes
Threshold sensitivity to a temperature drop at a level of +25° C	1°
Focusing range	500--1500 mm
Range of working temperatures	+10--+70° C
Working spectral range	1.8--4.8 μm
Inspection travel rate along the length of a product	10 mm/sec
The size of a horizontal record line	180 mm

The heat viewer is structurally designed in the form of two blocks: an optical head mounted on a self-propelled chassis, and a recording block. Both blocks are connected together by an electrical cable.

A general view of the device is shown in Figure 3. This instrument can also find application in the study of the heat field of the surfaces of various cylindrical products.

BIBLIOGRAPHY

1. Miroshnikov M.M., "Teoreticheskiye osnovy optiko-elektronnykh priborov" ["The Theoretical Principles of Optronic Devices"], Leningrad, Mashinostroyeniye Publishers, 1977, p 600.

2. Bykov V.M., ELEKTRICHESKIYE STANTSII [ELECTRICAL POWER STATIONS], 1977, No 5, p 31.

3. Miroshnikov M.M, et al., Patent No. 412825, BYUL. IZOBR. [BULLETIN OF INVENTIONS], 1976, No 29.

8225
CSO: 8144/976

PUBLICATIONS

UDC 539.1

TRANSFER OF ELECTRON-EXCITATION ENERGY IN CONDENSED MEDIA

Moscow PERENOS ENERGII ELEKTRONNOGO VOZBUZHDENIYA V KONDENSIROVANNYKH SREDAKH in Russian 1978 signed to press 13 Apr 78 pp 3-20

[Annotation, table of contents, preface and introduction from book by V. M. Agranovich and M. D. Galanin, Izdatel'stvo "Nauka," 4,000 copies, 383 pages]

[Text] This monograph is the first book in world literature dedicated to the sequential presentation of the basic results of theoretical investigations of the transfer of energy from electron excitation in condensed media. The special features of energy transfer in amorphous and crystalline media are considered in close relationship to their optical properties and, in particular, in relation to the effect of energy transfer on the luminescence characteristics. Various mechanisms of energy transfer are discussed (resonance transfer of excitations, excitons, radiation transfer), as well as special features of energy transfer at high excitation levels. The important role played by the energy transfer of electron excitation in the analysis of numerous optical, photoelectric radiation and other properties of crystals, solutions, biological substances, etc., is widely known.

This book is intended for scientific workers (physicists, chemists, biologists), as well as graduate students and upper classmen in these specialties who, in their investigations, encounter problems of energy transfer of electron excitation.

Table of Contents

Table of Contents (continued)

Table of Contents (Continued)

Table of contents (Continued)

Preface

Energy transfer of electron excitation in liquid and solid bodies is one of the most fundamental problems in condensed-state modern physics. This problem is universal since the energy of electron excitation is an intermediate process between the initial act of electron excitation and those final processes in which electron energy is utilized. In this connection, the study of mechanisms of electron energy, transfer and, in particular, the study of their efficiency is found to be necessary in investigating the interactions between various kinds of radiations and a substance in all those cases where one is interested not only in the very fact of absorption of radiation energy, but also in those phenomena that originate, in this case, in the absorbing medium.

Luminescence, radiation physics and radiation chemistry, photosynthesis, biochemistry and bioenergetics -- this is a far from comprehensive list of modern science areas where energy transfer of electron excitation is of principal importance.

In the last 30 years, along with investigations of liquid solutions, investigations of energy transfer of electron excitation developed most intensively in crystals. This was due not only to the general progress of the development of experimental and theoretical physics of solids, but also to numerous applications. In particular, energy transfer of electron excitation in crystals is used widely in developing various kinds of luminescent solids, scintillators and materials used in quantum electronics (laser crystals and solutions). One reason for the stimulation of wide investigations of energy migration of electron excitation in organic crystals is the presence of sensitized luminescence, as well as a possible role of energy migration in biological systems. These investigations are used in an attempt to answer a cardinal question for bioenergetics -- "how does energy control vital activity? How does it put a live machine in motion?" (Saint D'yerdi) [1].

The problem of electronic excitation energy transfer as a whole has become so broad and multifaceted that it is very difficult to reflect it in all its aspects. Therefore, the authors of this book do not pretend to have exhausted all sides of this problem. To a certain extent, the selection of the material presented is subjective. In choosing the material, we strove to cover, besides the theoretical bases, those problems which appear to be the most developed at present and are most frequently used for the interpretation of an experiment. On the other hand, we strove to indicate the limits of the applicability of the theory as well as to point out problems still unsolved. Regrettably, certain important areas of energy transfer investigations have still not been touched upon or touched upon only in the form of references to respective original papers. These areas include the effect of the magnetic field on transfer with the participation of triplet levels of organic molecules, transfer in biological systems and a great number of other, more special problems.

Excellent system models most frequently used for studying energy transfer are molecular liquids and molecular crystals, as well as crystals activated by rare-earth ions. The basic rules for energy transfer of electronic excitation known at present were discovered precisely by investigating the optical and photoelectric properties of these substances.

This monograph is dedicated to discussing the theoretical results obtained in such studies. Experimental data is used only in cases where it makes it possible to show how well the theory agrees with the experiment.

A fuller presentation of experimental investigations may be found in the monograph "Non-Radiation Transfer of Electron Excitation Energy" by Ye. N. Bodunov, V. L. Yermolayev, Ye. B. Sveshnikova and T. A. Shakhverdov.

The special features of energy transfer in amorphous and crystalline media are considered in close relation to their optical qualities and, in particular, in connection with the effect of energy transfer on the luminescence characteristic. Various mechanisms of energy transfer (resonant transfer of excitations, excitons, radiation transfer) are discussed, as are special features of energy transfer at high excitation levels.

Most of the problems touched upon in this book were practically untouched on in literature. Therefore, it is possible that there may be inaccuracies in the book. The authors will be grateful for any critical remarks which they hope to take into account in some form in the future.

We would like to express our special gratitude to those numerous Soviet and foreign colleagues who sent us copies of their papers. The authors are grateful to P. P. Feofilov for a number of criticisms which were taken into account in the final version of the manuscript.

Introduction

Energy transfer from excited atoms, ions and molecules to unexcited -- is a phenomenon occurring widely in nature. We encounter this phenomenon frequently when the concentration of interacting particles and the life of the excited state are great enough. The simplest and most graphic manifestation of energy transfer is attenuation of the luminescence occurring as a result of the interaction of excited and unexcited molecules or, conversely, the sensitization of luminescence, i.e., the origination of molecule luminescence previously unexcited.

In condensed media, phenomena related to energy transfer and deactivation of excited molecule were already discovered in early investigations of fluorescence in solutions of organic paints. It is precisely in these investigations that depolarization of luminescence and attenuation of its concentration, occurring when the concentration of the solution increases, as well as attenuation of luminescence by extraneous substances, were observed for the first time.

Originally, attempts were made to consider luminescence attenuation in liquid solutions analogous to the interaction between molecules or atoms in gases on the basis of a concept of "collisions of the second kind." This term, introduced at first for designating processes of collisions between excited atoms and electrons, accompanied by the changeover of excitation energy of atoms into the kinetic energy of the electrons, came to be used later for all processes leading to the deactivation of the excited state [2].

S. I. Vavilov first attempted to explain fluorescence attenuation of liquid solutions as a result of collisions of excited molecules with molecules of the attenuator [3]. This approach led to success in the case of fluorescence attenuation of solutions by extraneous colorless attenuators, especially after the special features of molecule motion in liquids were taken into account. As is well known, the number of collisions in ideal solutions is determined by the gas-kinetic formula and does not depend on viscosity. However, the statistic of collision in liquids differs from the statistic of collisions in gases -- collisions in liquids are not distributed uniformly, but follow in certain series. Since the first collision (so-called "meeting") already usually leads to attenuation, the kinetics of attenuation is determined by diffusion and, therefore, depends greatly on the viscosity of the solution. S. I. Vavilov was the first to turn his attention to this circumstance. The diffusion theory of attenuating luminescence by extraneous colorless attenuators, which he developed with B. Ya. Sveshnikov [4], based on Smolukhovskiy's theory of coagulation, agrees well with the experiment.

However, an attempt to apply similar concepts to concentrated attenuation and depolarization, originating under the effect of interaction between equal molecules, was found to be unsuccessful. The weak dependence of these phenomena on the viscosity of the solution indicated that under these conditions the short period of action taken into account in [3, 4] is not enough and, essentially, another approach is needed.

J. Perrin [5] was the first to suggest and later F. Perrin [6] suggested in greater detail that concentration phenomena in luminescent solutions may be explained by "molecular induction," i.e., remote acting interaction between the excited molecule and the unexcited one, similar to the interaction between classical electronic dipole oscillators. Within the framework of this attractive and basically correct idea there were not, however, taken into consideration the effects of relaxation that led to quantitatively wrong results.

In connection with the lack of a satisfactory microtheory of energy transfer, S. I. Vavilov, in his following papers [7] on concentration phenomena, proceeded along the way of building the phenomenological theory. He introduced the probability of transfer as an empirical value proportional to concentration. His idea was that concentration phenomena -- attenuation and depolarization -- are due to one and the same process of energy transfer. It was assumed thereby that attenuation occurs because part of the transfer acts is accompanied by deactivation of both interacting molecules ("transfers with attenuation"). Such a process appeared probable at one time in connection with the drop in luminescence output at anti-Stokes excitation [8] present in fluorescent solutions.

Subsequently, however, the viewpoint on concentration depolarization and concentration attenuation as a single process was not confirmed. As shown by V. L. Levshin [9], in a case of concentration attenuation, it is due to energy transfer from excited molecules to nonluminescent (or luminescent in another area of the spectrum) dimers. Nevertheless, S. I. Vavilov's ideas on the role of "inductive resonance" in energy transfer were fruitful and greatly stimulated experimental and theoretical investigations in which many important rules for energy transfer were later established. It has thus been shown that attenuation of luminescence by absorbing substances is related to the value of the overlapping of spectra [10]. The paper by P. P. Feofilov and B. Ya. Sveshnikov [11] established the relationship between attenuation and the period of the excitation state etc.

The first satisfactory theory of energy transfer in a condensed medium for molecules with broad spectra was developed by Forster [12]. This theory is based on the perturbation theory in the adiabatic approximation. It proposed that energy transfer occurs due to weak dipole-dipole interaction between molecules. The interaction is assumed to be so weak that it does not change the initial optical spectra of the molecules. Under these conditions, Forster was able to show that the probability of energy transfer can actually be expressed by the integral of luminescence spectra overlapping and absorption of interacting molecules.

Forster was also the first to average probabilities of transfer in accordance with the totality of molecules in the solid solution and obtain formulas that could be substantiated by experiments. Forster's theory preserved its full importance and is borne out by experiments in cases where conditions for its applicability are fulfilled.

Subsequently Forster's theory was generalized in the paper by Dexter [13] for cases of multipole and exchange interactions. Its further development consisted of taking into consideration various complicating circumstances such as, for example, the diffusion motion during the lifetime of the excited state. In view of the fact that Forster's theory is an approximation, limits for its applicability were discussed many times in the following years. In particular, in [8] in using the classical model of two dipole oscillators with friction, Forster's formula was obtained only to such an approximation where the lifetime of excitation in the acceptor is many times less than the time of the reverse transfer. Robinson and Frosch [14] came to a similar conclusion within the framework of quantum-mechanical considerations. Forster himself discussed the applicability conditions of his theory [45]. He produced a classification of interaction types, according to which his initial theory applies to the case of a "very weak relationship."

The question of the applicability limits of Forster's theory was also considered in a great number of papers which used the matrix density method. It is precisely in these papers that the role of relaxation processes and energy transfer phenomena are clarified most fully, and clear-cut criteria for the applicability of those or other approximations are given (see further Chap. 1).

Thus, the elementary act of "inductive-resonance" energy transfer is considered as the result of weak interaction between two molecules -- a donor and an acceptor of energy. The effects of energy transfer observed in the experiment, for example, sensitization or attenuation of luminescence, may be considered a result of action of independent elementary acts of transfer. This concept is correct for sufficiently diluted solutions in an optically inert transparent solvent.

As a rule, impurity molecules in the solution form a spatially disordered system. Therefore, the excitation energy of the impurity and the energy of its resonance interaction with the environment are random values, generally speaking, different for various impurity centers. As a result, the analysis of the problem of energy transfer of electronic excitation to molecules of the impurity is essentially complicated relating it, in principle, to the problem of electrical conductivity of spatially disordered media [150].

This aspect of energy transfer to impurity molecules in crystals becomes especially important at low temperatures and in cases where the nonuniform width of the impurity absorption line is great, not only as compared to its uniform width, but also exceeds the energy of resonance interaction between the impurity molecules at an average distance between them. In this case, in particular, nonresonance processes of energy transfer, accompanied by generation or destruction of phonons of the lattice or by an other of its elementary excitations, are also essential. It is precisely these kinds of processes that destroy the localization of states in disordered media and make it possible to transfer energy to impurity molecules at fairly low concentrations of the impurity, predicted by Anderson in 1958 (Chap. V, section 9).

An essentially different physical picture of energy transfer of electron excitation originates in crystals where, due to the translation symmetry, excitation is possible of any elementary cell of the crystal or of any of the component crystals of the molecules. As is well known, in this case, energy transfer may be due to the motion of quasi-particles -- excitons. The fundamental idea of excitons put forth in 1931 by Ya. I. Frenkel' [15], which plays such a great role in the modern physics of solids, is related directly also to the energy transfer mechanism in crystals. This was especially clearly realized in 1938 when Frank and Teller, in an article entitled "Migration and photochemical action of excitation energy in crystals" [16] for the first time posed the question on how the energy, absorbed by some cell in the crystal, can migrate in the crystal and then can be utilized for a photochemical or some other process at any other fairly removed point. In this connection, it is stressed in [16] that a "crystal consists of identical elementary cells formed by atoms, molecules or groups of atoms, molecules or ions. If the crystal is excited, the excitation may be localized in any of these elementary cells. Such localized excitation does not conform to a stationary state. The relationship between particles in the crystal and resonance, due to the identity of elementary cells, will lead to the excitation energy migrating from one cell to another." Qualitative discussions in [16] based on results of investigations by Ya. I. Frenkel' [15] and Peierls [17] touch upon many problems, to some extent, of nonradiational energy transfer of electron excitation in crystals which also remain urgent at present. In [16], energy transfer by wave packets, as well as energy transfer by localized (noncoherent) excitons are talked about. In the latter case, thermo-activated transitions, as well as the tunnel effect (at low temperatures) are indicated as the causes for exciton migrations. Although in the characteristic of exciton propagation in the crystal, the words "diffusion process" are used only for incoherent excitons; for wave packets there is also used the concept of the length of the free path and the strong change in the direction of motion of the exciton (but not its energy) which must originate when excitons are scattered by phonons. Also a number of statements is made in [16] on the mechanism of interaction between excitons, crystal defects and its surface and, in particular, on the mechanism of trapping an exciton by foreign molecules. Thus, Frank and Teller [16] actually formulated an entire program of theoretical investigations.

In about the same years, intensive experimental investigations of energy transfer in crystals began. In particular, Bowen [18] undertook, for the first time, a broad study of the effect of small amounts of impurities on the luminescence of molecular crystals. He showed that luminescence of crystals is subjected mostly to the effect of impurities that absorb light strongly in the spectrum area of pure crystal luminescence. The presence of such impurities reduces the luminescence intensity of the basic substance and the reduction in intensity is accompanied by a reduction in the length of the drop in the glow of the crystal. Bowen stressed that the nonradiation transfer mechanism plays the basic role, i.e., the mechanism that does not accompany the formation of luminescence photons of the basic substance.

The first experiments on energy transfer by excitons in halide-alkaline crystals were made by Apker and Taft [19]. They observed the transfer of energy by excitons to F-centers (for later experiments on halide-alkaline crystals, see [20], [21]). The results of investigations of the mobilities of excitons in crystals of inert gases (Ne, Ar, Xe) obtained recently are cited in [22].

The mobility of excitons in semiconductor crystals (Van'ye-Motta excitons), due to small effective masses and comparatively weak exciton-phonon interaction, was found to be so high (the diffusion coefficient for excitons for some crystals reaches a value in the order of $D \approx 10^3 cm^2/sec$; for comparison we will indicate the value of the diffusion coefficient for singlet excitons in anthracene $D \approx 3 \times 10^{-3} cm^2/sec$), that its study required using special methods [23]. Successful measurements of D in semiconductors were made only recently in connection with the investigation of their luminescence at high concentrations of excitons.

Energy transfer in semiconductors is made by coherent excitons (diffusion of wave packets). In such crystals, due to the macroscopically large values of the Bohr radii of excitons ($r_B^{-3} \approx 50$ to 100A), already at concentrations of excitons $N \lesssim r_B^{-3} \approx 10^{18} 1/cm^3$, an entire series of new phenomena is observed (biexcitons, electron-hole drops), the study of which constitutes at present an entirely new direction of semiconductor physics [24]. In particular, in investigating the phenomena mentioned, not only the mobility of individual excitons becomes urgent, but also the mobility of various kinds of exciton complexes (for example, electron-hole drops), effects of interactions between these complexes etc. [25]. Some of the results discussed in this book may also be used to characterize the properties of the Van'ye-Motta excitons (for example, the temperature dependence of the diffusion coefficient, individual problems of kinetics and luminescence of excitons). Moreover, to stress the nature of problems originating thereby, special features of the growth of electron-hole drops in germanium are discussed in somewhat greater detail (in Chap. 6). However, a full discussion of the collective properties of excitons, biexcitons, electron-hole drops and other possible exciton complexes is beyond the scope of this book and will require, without doubt, the writing of special reviews and monographs.

Returning to the theory of exciton energy transfer in molecular and ion crystals, we will note that at first this theory developed, to a certain extent, independently of the theory of energy transfer between molecules in solutions. Only much later, at the end of the fifties, was the closest tie between them realized to the full extent.

Concepts on the diffusion nature of exciton motion were used for the first time in a paper by Yu. I. Karkhanin and V. Ye. Lashkarev [26] for interpreting experiments (for calculating the relationship between the intensity of surface annihilation of excitons in Cu_2O and absorption coefficient of the exciting light k); in a paper by A. N. Faydysh [27] for calculating the dependence on k of the speed of trapping excitons in molecular crystals [28] by impurities; as well as in paper [29] (when evaluating for anthracene

controlled by diffusion of excitons the speed of their trapping by naphthacene, see Chap. 7). Later, in [30], [31], there was formulated a more general integral-differential equation for exciton concentration in which, along with exciton diffusion, account was also taken of the change in their concentration due to reabsorption of the luminescence light.

The idea of exciton diffusion was found to be very fruitful and describing exciton migration in the diffusion approximation was justified in most cases. At present, in spite of the difference noted in the transfer mechanisms in solutions and crystals, their common nature became clear to a considerably greater degree. This common nature consists not only of the fact that an elementary act of transfer is due frequently, in this or another case, by one and the same type of interaction (for example, dipole-dipole), but also by the fact that there is a continuous transition from cases of transfer molecule-donor -- molecule acceptor in solutions to the case of energy migration along identical molecules in solutions and, finally, to migration of excitons in a crystal. The diffusion approach spans not only considering the diffusion of molecules in a solution, but also the diffusion of excitations along molecules, as well as diffusion of excitons. Finally, the concept of energy transfer by coherent and incoherent excitons corresponds (according to Forster) to cases of strong and weak interaction between molecules.

The concept of the contents of this book can be obtained by the reader by acquainting himself with the table of contents and leafing through the book rapidly. Here, therefore, we will limit ourselves only to several remarks.

The first two chapters of the book are dedicated basically to the theory of energy transfer in solutions. In particular, the first chapter considers an elementary act of energy transfer between two interacting molecular systems located at a given distance from each other. In this, and a number of other chapters, the authors strove to simplify the presentation as much as possible in order to make clear the physical bases of the theory. At the same time, we considered it advisable to utilize in the first chapter the concept of a density matrix as applied to a two-level system,i.e., the approach which became popular in connection with the development of quantum electronics. In spite of the primitive initial model, this approach makes it possible to understand the physical essence of various approximations in the theory and make rough, but realistic evaluations of the order of magnitude of the probability value of energy transfer.

The first chapter also presents Forster's theory which, as already noted, played a most important role in the development of the entire energy transfer problem.

The second chapter considers methods and results of averaging the probability of transfer according to the totality of molecules of energy donors and acceptors. In this chapter, Forster's result is reproduced as well as certain of its refinements. Also presented in detail is the theory that takes into account the effect of molecular motion in a liquid solution. Of the huge

number of experiments in which energy transfer in solutions was investigated, the second chapter shows only examples of several measurements which indicate how well the theory is confirmed by experiment, if conditions of applicability of the theory are met and the necessary experimental precautions are observed.

Chaps. 3 to 8 are dedicated to energy transfer in crystals. These chapters contain a discussion of the relationships between experimentally measured physical values and those microscopic characteristics of the crystal which, in the final result, determine the intensity of the processes of energy transfer of electronic excitation in crystals.

How, on the basis of experimental data of energy transfer in crystals, can one judge which excitons (coherent or incoherent) make the basic contribution to the energy transfer? How to find the diffusion coefficient of excitons in this or another crystal? What is the mechanism of interaction between excitons and impurities and division boundaries of media? What is the role of radiation transfer? What are the special features of energy transfer between impurity molecules in crystals and what is the role of the matrix in this case?

This is a partial list of questions which must be answered to some approximation in deriving the above-mentioned correlations. Chapters 3 to 8 of this book are basically dedicated to discussing these.

In particular, Chap. 3 considers using the method of an active field, the effect of the crystalline matrix on the energy of the resonance interaction of the impurity molecules with each other which leads to a nonradiational energy transfer of electronic excitation between them. If the distance between impurity molecules is great compared to the size of the elementary cell of the crystal, the effect of the matrix on the energy of the resonance interaction is determined mainly by the permittivity of the medium. In this connection, calculations of the energy of resonance interaction between the molecules of the impurity as well as calculations of the tensor of the permittivity of the matrix are found to be inseparably tied together as shown in Chap. 3. Since, on the other hand, the permittivity tensor determines the optical properties of the medium, the above-mentioned nature of the presentation makes it possible to trace sequentially the relationship between the speed of nonradiational energy transfer among molecules of the impurity and optical properties of the matrix and, in particular, the structure of its exciton spectra.

Chapter 4 contains the presentation of those individual results of the exciton theory (for example, the problem of exciton-phonon interaction is discussed), which are used in Chap. 5 for calculating their kinetic parameters that determine the speed of energy transfer. Also discussed are the properties of biphonon and exciton states, the presence of which, generally speaking, may affect the kinetics of collisions between quasi-particles (in particular, the speed of bimolecular annihilation of excitons). Moreover, in Chap.4 is sequentially developed a microscopic theory of electron excitation energy transfer between impurity molecules which makes it possible to trace the effect of virtual excitons on the speed of transfer as well as to take into

account the effects of resonance interaction between the impurity molecules and the matrix.

In the exciton area of the spectrum, electronic excitations -- excitons and quanta of the electromagnetic field in many crystals and, in particular, in many luminescent crystals interact so strongly, unlike gases or vapors, that in order to describe correctly their properties (mobility, luminescence and absorption spectra) at low temperatures,it is more adequate to use concepts,, not of excitons or photon, but polaritons, i.e., quasi-particles originating at strong exciton-photon interaction. In this connection, Chap. 4 shows how the use of these concepts makes it possible to tie-in within the framework of a single physical picture a rather wide circle of phenomena such as, for example, the nonradiational and radiational energy transfer of electron excitation, exciton absorption and luminescence etc.

Chapter 5 is dedicated to the theory of the mobility of excitons and the theory of their interaction with molecules of the impurity and with each other. Also discussed in this chapter are the special features of energy transfer of electron excitation, along the impurity molecules, Anderson's localizations of excitations and nonresonance processes. In Chap. 5,the basic attention is concentrated on calculations of respective kinetic parameters which, in Chap. 6, where the phenomenological theory of exciton migrations is developed, are assumed to be already given. It is precisely the results of the phenomenological theory that are usually compared with experimental data,and the values of kinematic parameters are determined on the basis of such a comparison. In this connection, in Chap. 6, there is made a calculation of experimentally determined values such as, for example, the quantum output of luminescence and the time of its attenuation, the quantum output of sensitized luminescence etc.

A review of the results of the experimental investigation of energy transfer by excitons is given in Chap. 7. This chapter is basically devoted to a comparison with the theories of radiational and nonradiational energy transfer, in particular, of that experimental data which may be used for the evaluation of kinetic parameters and, in particular, for the evaluation of the diffusion coefficient of excitons and its temperature dependence. It is precisely according to the nature of this dependence (Chap. 4) that it is possible to judge whether coherent or incoherent ("localized") excitons transfer the energy in this or another crystal, in other words, is diffusion of wave packets or diffusion in accordance with a model of random transitions of excitations along the nodes of the lattice taking place.

Chapter 8, the last, discusses physical phenomena which may occur due to the interaction between excitons at the boundary of the crystal and attenuating excitons on the metal surface. In a certain sense, questions and situations originating here are very similar to those discussed in Chap. 4 when analyzing the mechanism of interaction between the exciton and the attenuating impurity (there -- excitons localized in the impurity, here -- excitons localized at the boundary between media etc.). At the same time, when analyzing metal

attenuation, a number of interesting possibilities open up. Thus, by the speed of metal attenuation of excitons it is possible to judge not only the value of the diffusion coefficient of excitons and the nature of its motion, but also electron rearrangements on the dielectric-metal boundary, capable of forming a "dead zone" etc. This direction of investigations of energy transfer by excitons (energy transfer to the surface) is still in the initial stage of its development and, we hope that the discussion here of problems related to this direction will stimulate the formulation of further investigations.

2291
CSO: 1870 END